European Journal of Aquatic Sciences
Vol 4 | Issue 2 | September 2025
ISSN 2976-7423

RESEARCH ARTICLE

Seagrass Water Temperature, Light Intensity and Sediment Phosphorus Mathematical Solutions for Estuary Management

Bruce R. Hodgson*

ABSTRACT

The aim of this study was to apply *Zostera capricorni* growth rate mathematical solutions to saline coastal lagoons to generate novel mathematical insights that could be used by estuary managers in other estuaries and saline lagoons. It is proposed that the quadratic curvilinear 2nd Order relationships of seagrass growth rates with water temperature and subsurface light intensity, and with linear relationships for sediment total phosphorus, have the potential to inform catchment runoff management strategies by applying the equations to similar data obtained for other *Zostera* species in coastal lagoons and estuaries. The equation for water temperature includes an expected 1.4°C increase due to climate change in the seagrass beds, which was consistent with the derived water temperature equation. Thus, the detailed data and information obtained from the online and published studies of *Zostera* provided important biological processes for assessing the likely effects of the three main environmental drivers on seagrass growth rates. Analysis of the data determined the optimum temperature, light intensity thresholds before photo-inhibition, and a benchmark for sediment total phosphorus (TP) associated with growth rates and higher and more stable biomass in the urbanized areas of the studied lagoon system. The relationship between Zostera biomass and TP indicates the possible optimization of seagrass biomass by catchment nutrient runoff.

Keywords: Biomass growth rate relationship with sediment total phosphorus, mathematical solutions for seagrass estuary managers, *Zostera* net growth rate curvilinear relationships.

Submitted: June 17, 2025

Published: September 04, 2025

10.24018/ejaqua.2025.4.2.30

Faculty of Science and Engineering, Southern Cross University, Lismore, New South Wales, Australia.

Corresponding Author:
e-mail: bruce.hodgson@scu.edu.au

1. Introduction

Seagrass management in estuaries is important for maintaining fish harvests (Unsworth *et al*., 2018) as recommended by the combined FAO and United Nations Environment Programme on Ecosystem Restoration (FAO, 2022). Accordingly, the aim of this paper is to develop equations for the various seagrass processes that could be used by estuary managers to maintain species of *Zostera* in urbanized estuaries and coastal lagoons. The fundamental processes involved are expected to allow estuary managers to apply their seagrass data to the same types of curvilinear equations derived here. The basic framework of the study is that the main drivers of seagrass growth rates are water temperature, subsurface light intensities, and sediment nutrient concentrations (Lee *et al*., 2007). The detection of seagrass changes in estuaries is often undertaken by monitoring the area and/or biomass (Cabaço *et al*., 2007), with controls on catchment sediment and nutrient load inputs (Lillebø *et al*., 2005). At times, the monitoring is supplemented by seagrass models to assist estuary managers in identifying key processes that may affect seagrass abundance (Neckles *et al*., 2012). They suggested monitoring should include the environmental variables used in seagrass models to aid management decisions. However, the review by de Boer (2007) showed seagrass models are multidisciplinary, requiring specialists to use them, and they also had knowledge gaps. In addition, model complexity may occur by including a large number of variables (see Scalpone *et al*., 2020; Thomas *et al*., 2005), thereby limiting the use of models by estuary managers. Therefore, to minimize complexity, the relationships derived here are curvilinear equations

for *Zostera* growth rates with water temperature and light intensity and linear for sediment total phosphorus with biomass. The seasonal variation of biomass at the Lake Munmorah sampling site, and long-term biomass changes in the whole of Lake Munmorah were assessed by Stability Charts derived from the study by Carr *et al*. (2012). As the equations used to describe relationships of *Zostera capricorni* biomass and growth rates are novel, being derived from curvilinear relationships in previous studies, the theoretical basis for the derivation of the equations is described here in Sections 1.1–1.3 as a precursor to the Methods, below. Note that a separate literature review section is not used because the literature relating to the theoretical aspects of *Zostera* growth rates is shown in the Introduction, the sections below, and in the Discussion.

1.1. Water Temperature and Zostera Growth Rate Theory

The literature on temperature models for *Zostera* species growth rate production is often uncertain for theoretical relationships with water temperature (Collier *et al*., 2017, see their Figure 3). Hence, to minimise complexity, the model-selection criteria were based on published studies of the effects of water temperature on growth rate. The uncertainty of the resulting curvilinear model was verified by assessing the R^2 and error bar values of the finally derived relationships. It is well known the optimum temperature for seagrass growth is around the peak of a mounded curve (see Figure 1e in Fong *et al*., 1997), so a theoretical curvilinear relationship of net growth rate with temperature was derived by the leaf marking method used by Holland (1982), which is supported by observations for *Zostera marina* (see Figure 2 in Moore *et al*. 1996). In addition, the gross growth rate was found to be linearly related to temperature by Kaldy (2014), so that relationship was derived using net growth rate data from Holland (1982). The *Zostera* leaf net growth rate, G_{net}, with water temperature, T°C, was investigated by the study by Scalpone *et al*. (2020), which confirmed using a curvilinear quadratic relationship, supported by their finding that water temperature limits seagrass growth with an optimal temperature, given by a balance of production with respiration. A curvilinear relationship of growth rate with water temperature was also confirmed by Dennison and Alberte (1985), which gives the mathematical solution by gross growth rate, $G_{gross,}$ minus the respiration rate R, that is the net growth rate, $G_{net} = G_{gross} - R$, in units mg gdw^{-1} day^{-1}. The respiration rate has an exponential increase with temperature of the form $R = a \times e^{bT}$, were "a" and "b" are constants for the seagrass species being modelled (see Figure 3 in Short, 1980), which was confirmed by Plus *et al*. (2003: Figure 4 by $R = 19.14 \times e^{(0.11 \times T)}$), where R is the respiration rate and T is the water temperature. Furthermore, Scalpone *et al*. (2020) indicated the optimum temperature, T_{opt}, occurs at the temperature where the respiration rate equals the net growth rate, G_{net}. Hence, G_{net} is expected to decrease at temperatures higher than T_{opt} because R continues to exponentially increase at water temperatures higher than T_{opt}, thereby giving a curvilinear relationship. That was confirmed by the global review by Nguyen *et al*. (2021, their Figure 2), which shows seagrass growth rates decrease with increasing respiration rates for twenty-four seagrass species in their Figure 4, including *Zostera capricorni*.

1.2. Light Intensity and Zostera Growth Rate Theory

The increase in *Zostera* net growth rate production with light intensity is asymptotic to the maximum growth rate, but photo-inhibition decreases photosynthesis at high light intensities in *Zostera marina* (see Short, 1980: Figure 4). More recently, Beer and Björk (2000) found *Halodule wrightii* had gross photosynthesis curvilinear with the irradiance light intensity, while Campbell *et al*. (2008, see their Figure 3) showed a curvilinear relationship of photosynthesis with light intensity due to photo-inhibition to begin at about 1200 µmol photon m^{-2} sec^{-1} for three seagrass *Halophila* spp. That was confirmed by Zhang *et al*. (2022, their Figure 2), who found a curvilinear relationship of *Zostera marina* productivity with light intensity duration. Similarly, photo-inhibition measured at 0.5 m depth inside the *Zostera capricorni* bed by Holland (1982) in The Tuggerah Lakes, caused a curvilinear relationship of growth rate with light intensity. On the basis of the literature, a curvilinear relationship of growth rate with light intensity was statistically tested using the data from Holland (1982).

1.3. Sediment Total Phosphorus and Zostera Biomass Relationship Theory

The seagrass growth rate with sediment phosphorus concentrations by Fong *et al*. (1997, see their Figure 1c) increases approximately linearly up to a maximum and then levels out. However, Harris (1977) only measured the *Zostera capricorni* biomass and found a linear relationship with sediment total phosphorus concentrations in the Lake Illawarra coastal lagoon. As the data in Holland (1982) and from Harris (1977) are from nearby lagoons, the Lake Illawarra data and relationship were assumed to apply to Lake Munmorah in the Tuggerah Lakes used by Holland (1982).

1.4. Application of Curvilinear Relationships to Seagrass Species in Estuaries and Saline Coastal Lagoons

The literature shows that the derived equations based on the results in Holland (1982) and Harris (1977) are valid and could be applied to other seagrass species in estuaries and coastal lagoons. The above literature shows that many seagrass species have curvilinear relationships. For example, the study by Collier *et al*. (2017, their Figure 4) showed *Zostera muelleri* (subspecies of *Z. capricorni*), *Cymodocea Serrulata* and *Halodule* uninervis had a curvilinear relationship with net productivity (equivalent to net growth rate in Holland (1982). In addition, Campbell *et al*. (2008) showed the seagrass species of *Halophila spinulosa, Halophila decipiens, Halophila ovalis, Cymodocea serrulata*, and *Syringodium isoetifolium* had curvilinear relationships of photosynthesis with light intensity. That suggests related species in other estuaries and saline coastal lagoons may have similar relationships to 2nd Order curvilinear obtained using data in Holland (1982). For example, the online literature shows *Cymodocea serrulata* is in the family Cymodoceaceae and has 16 seagrass species in tropical and subtropical coastal waters. The common seagrasses

are *Syringodium isoetifolium, Cymodocea nodosa, Halodule uninervis, and Cymodocea rotundata*, and in the tropical and subtropical Indo-Pacific is *Syringodium isoetifolium*. Hence, the curvilinear relationships of these seagrass species in estuaries and saline coastal lagoons is worthy of further research. The literatures supporting these equations are shown in the methods and the references for key findings are shown in the Discussion.

2. Methods

The sampling sites and data for this investigation are from Holland (1982) in Lake Munmorah, part of the Tuggerah Lakes coastal lagoon, in New South Wales (NSW), Australia (including Lake Munmorah 33°13′04.8″ S, 151°34′08.0″ E, Lake Budgewoi 33°14′38.8″ S, 151°31′51.0″ E and Tuggerah Lake 33°17′50.2″ S, 151°29′53.7″ E). The study area is described in *Chapter 2* of Holland (1982) as having brackish salinities 20.1 to 32.2 $^{0}/_{00}$ at the time of sampling and fringing marine seagrasses around the entire shoreline, including small areas of *Halophila ovalis* and *Ruppia megacarpa*, with three interconnected lakes and the oceanic connection in the largest, Lake Tuggerah. The study by Harris (1977) on *Zostera* biomass was undertaken in Lake Illawarra (34°32′32.2″ S, 150°49′32.8″ E), about 160 Km south of Lake Munmorah (see Figure 1 in Hodgson & Bucher, 2023) and the lake is described in Harris (1977) *Chapter 1.2.2 "The Study Area" and Figure 1.2, page 11*. The lake has a fringing vegetation of *Zostera* with some *Ruppia megaacarpa*, salinity 29.5 to 33.8 $^{o}/_{oo}$ and a single oceanic connection; see Harris (1977, Figure 3.9, page 100). Note that the name *Zostera capricorni* is used to be consistent with the literature data used for this study. Although the species *Z. muelleri* is present, it was confirmed by Harris (1977) as only in small amounts, and is now considered a subspecies of *Zostera* (Chartrand *et al*., 2016).

The detailed field data from Harris (1977) and Holland (1982) in coastal lagoons were collated and analysed for their growth rates, water temperature, and light intensity conditions inside a *Zostera capricorni* seagrass bed. Note that the use of historical data was verified by comparison with recent seagrass publications. The necessary estimations and adjustments can be fully verified with access to the original raw data in the internet links after Table I and in the references for Harris (1977) https://doi.org/10.26190/unsworks/20231 and Holland (1982) https://doi.org/10.26190/unsworks/7044. Hence, optimising of the equations to describe the various effects of the main seagrass drivers are shown in the Results section, below. That involved the process of evaluating the performance and validity of the possible models available in the literature that gave reliable predictions. To do that, the selection of the best model from variations in curvilinear was tested using statistical comparisons of different possible relationships, and the parsimonious, i.e., sparing of complexity, showed the best-fitting model was a 2nd Order Polynomial. Hence, it was not necessary to use Bayesian Information Criterion (BIC) to select the best-fitting statistical model among models in the literature because the 2nd Order curvilinear polynomial type was obtained by trying various types of balancing possible models to fit the literature and available data with minimum complexity. Furthermore, those early studies by Harris (1977) and Holland (1982) were undertaken as part of major investigations on the ecology and biological processes of *Zostera* in saline coastal lagoons in New South Wales (NSW), Australia, and continued by others for *Z. capricorni* and other *Zostera* and related seagrass species to 2019 (see Hodgson & Bucher, 2023 and references therein). By providing that foundation of biological processes in the coastal lagoons, the equations were also used for assessing the recent effects on *Zostera* growth rates with water temperature increases due to climate change.

2.1. Data Used in the Study from Published Online Sources

The light and water temperature are shown in *Attachment Al* (note *A1* was altered to *Al* i.e., 'lower case L') and is described in Holland (1982): *Chapter 2* and *Zostera* growth rates in *Chapter 4* undertaken at an inshore site in 1.0 m water depth called Munmorah Flats, MF, in the northwest of Lake Munmorah (Holland, 1982: *Figure 6.1*). The site was selected with a low catchment population, so the effects of water temperature and light conditions showed natural changes in healthy areas of *Zostera* without effects of the moderate nutrient inputs. Eleven net growth rate measurements in response to temperature and light conditions were undertaken over a 17-month period from October 1978 to February 1980. The incident light intensities, I_0, at 0.5 m above the water surface and the light intensity at 0.5 m inside the *Zostera* bed, I_d, were measured by Holland (1982) with a Li-Cor quantum sensor measuring photosynthetically active radiation (PAR) units of radiation (μmol m^{-2} sec^{-1}). Thermal effects on seagrass growth rates were measured in the laboratory at low light by Holland (1982, *Table 6.6* "*Growth rates of Zostera shoots after a range of exposure times*") by measuring the thermal reduction in growth rates at fixed water temperatures over time (see Section 3.5.1).

Holland (1982) used the leaf marking method in the field, which assesses growth directly and only requires measurement of the leaf loss rate, L (Verhagen & Nienhuis, 1983), rather than the respiration rate required by the oxygen evolution method. The leaf growth rate was measured by the increase in leaf length biomass using the "Increase in Plant Tissue method", called here net growth rate, G_{net}. Note that the net growth rates have units of mg gdw^{-1} day^{-1}, called "comparative growth rates" by Holland (1982), which are equivalent to the nomenclature for seagrass production in the literature. The *Zostera* biomass was calculated by the monthly average shoot weight multiplied by the shoot frequency in Holland (1982), *Chapter 5, Table 5.2*.

Leaf loss rates are an important part of seagrass processes. It was noted by Moore *et al*. (1996) that leaf loss rates were highest in summer, indicating the loss rates are related to temperature, so the relationship of loss rates with water temperature was derived using the *Zostera* percentage viability data in Holland (1982). To derive that relationship, loss rates were estimated using the percentage viability of the *Zostera* leaves, measured in relation to the

TABLE I: The Data Source Summary Table Lists Functional *Zostera Capricorni* Characteristics with Derived Relationships from Referenced Data Sources

Functional characteristics	Description	Units	Derived equations	Source of data*
		Zostera and environmental data in Holland (1982).		
Water temperature	Seasonal variation	°C	Eq. (1)	*Appendix Al: "Temperatures at the four field sites: November 1978 through February 1980"*, page 194. Temperatures in October, 1978, and January, 1979 from *Figure 2.4*: "*Seasonal variation in water temperature at four field sites in Lakes Munmorah and Budgewoi Munmorah Flats*."
Gross growth rates	Gross growth rate relationship with water temperature	mg gdw^{-1} day^{-1}, °C	Eq. (2)	Derived $G_{gross} = G_{net}$ + Loss rate (Table II) and water temperatures from *Appendix Al*
Loss rate	Loss rate relationship with temperature	mg gdw^{-1} day^{-1}, °C	Eq. (3)	*Appendix A4* "*Percentage Viability Lake Budgewoi Test Sites. Includes Munmorah Flats.*", November, January and September, 1979 viability estimated from *Figure 6.2:* "*Percentage viability of Zostera at the four field sites: Munmorah Flats*" multiplied by *Table 6.1* net growth rates.
Net growth rate	Seasonal variation net growth rate, G_{net}	mg gdw^{-1} day^{-1}		*Table 6.1* "*Comparative Growth Rates of Zostera capricorni: Field Sites.*" is called here net growth rate
Net growth rate alternate method	Net growth rate = Gross growth rate (Eq. (2)) – Loss rate (Eq. (3))	mg gdw^{-1} day^{-1}	Eq. (4)	See derivation of (2) in Fig. 3 and (3) in Fig. 4.
Net growth and optimum temperature	Net growth rate quadratic relationship with temperature	mg gdw^{-1} day^{-1}, °C	Eq. (5)	*Table 6.1* net growth rate and water temperatures in *Appendix Al*, page 194, with net rate at highest measured 26.6°C in November, 1978, and expected highest 28.0°C by eq. 4
Respiration rate	Respiration rate at optimum temperature	mg gdw^{-1} day^{-1}, °C	Eq. (6)	See derivation in Fig. 6.
Incident light intensities	Seasonal variation in incident light intensities, I_0	µmol m^{-2} $sec^{-1.}$	Eq. (7)	*Table 2.2 "Incident light intensity: November, 1978 - February, 1980."* and January, 1979 from *Figure 2.7* "*Seasonal variation in percentage light penetration at the four field sites.*",
Zostera bed light intensities	Monthly variation of light intensities at 0.5 m inside the *Zostera* bed, I_d	µmol m^{-2} sec^{-1}	Eq. (8)	Light intensity at I_d 0.5 m by I_0 x% % light penetration from *Table 2.2* "*Incident light intensity: November, 1978 - February, 1980*" and Appendix *Al*: "*Percentage penetration of incident light at the four field sites. Including Munmorah Flats*" page 196. Estimates and adjustments in Table II.
Zostera bed light with incident light	Relationship light intensities at 0.5 m inside the *Zostera* bed with incident light intensity	µmol m^{-2} sec^{-1}	Eq. (9)	*Table 2.2* and *Appendix Al page 196*.
Net growth rate and light	Net growth rate quadratic relationship with light intensity at 0.5m depth in the *Zostera* bed	mg gdw^{-1} day^{-1}, µmol m^{-2} $sec^{-1.}$	Eq. (10)	*Table 6.1* net growth rate and Light intensity at 0.5 m in Table II.
Zostera biomass with G_{net}	*Zostera capricorni* biomass relationship with net growth rate	g dw m^{-2}, mg gdw^{-1} day^{-1}	Eq. (11)	Biomass *Table 5.2* "*Zostera capricorni reproductive shoots: shoot weight, frequency and biomass*" with Table 6.1 "*net growth rate.*"
		Zostera and sediment total phosphorus data in Harris (1977)		
Zostera biomass with total phosphorus	*Zostera* leaf biomass and sediment total phosphorus relationship	g dw m^{-2}, μg^{-gdw}	Eq. (12)	Biomass Tables A4.1, A4.2, and A3.5 not including sites affected by light limitations. Total Phosphorus Tables A2.2, A2.3 and A2.4

Note: * The data used to derive those relationships are shown in the online links: Holland (1982). The effects of some environmental factors on the growth and viability of *Zostera capricorni* Asherson. M.Sc. Thesis, School of Botany, University of New South Wales. https://doi.org/10.26190/unsworks/7044. Harris, M. McD. (1977). Ecological Studies on Illawarra Lake with Special Reference to *Zostera capricorni* Ascherson. Master of Science Thesis, School of Botany, University of New South Wales, Sydney, Australia. https://doi.org/10.26190/unsworks/20231.

net rates, from *Appendix A4* "*Percentage Viability*". The Loss rates were estimated by ([1 - % 1%-viability/100] x *Table 6.1* "net growth rate") mg gdw^{-1} day^{-1}, shown in Table II. The loss rates allowed estimation of the gross growth rates, G_{gross}, by $G_{gross} = G_{net}$ (from *Table 6.1*) + L, and the estimated gross growth rates are also shown in

TABLE II: Estimated, Adjusted (square brackets) and Estimated not Sampled (bold) G_{NET}, Loss Rates, G_{GROSS}, Incident Light Intensities, I_0, Percentage I_0 in *Zostera* Bed, Resulting Intensities in Bed, I_D, and Biomass Derived from Measured (in italics) Water Temperatures, *Appendix Al Page 194* and Estimated from *Figure 2.4*, Net Growth Rates, *Table 6.1* and G_{GROSS} - L, Incident I_0, *Table 2.2* or Back Estimated from % Penetration in *Zostera* Bed, Appendix *Al Page 196*, and Biomass, *Table 5.2*, from Holland (1982)

Month from Oct. 1978	Date	Water Temperature °C (Italics not in Appendix Al)	Estimated net growth rates, $G_{net,}$[a] (G_{gross} - L)	Loss rates, L,[b]	Gross growth rates G_{gross}[c]	Incident light intensities, I_0[d] and Est. (100 × I_d/% penetration)	% Light intensity reaching 0.5 m[e]	Light intensity 0.5 m inside *Zostera capricorni* bed, I_d[f]	Biomass, B[g] *measured*
1	Oct-78	*19.6*	*12.8*	1.7	14.5	**2124**	**66.5**	**1414**	*26.9* [18.5]
2	Nov-78	26.6	**10.4**	**11.7**	**22.1**	*2282*	*67.3*	1536	**12.4**
3	Dec-78	22.5	*12.8*	5.1 [4.1]	16.9	*2140*	*68.6*	1468	*21.2*
4	Jan-79	*26.3*	**10.9**	**11.0**	**21.9**	**2021**	**66.3**	**1340**	**10.6**
5	Feb-79	26.5	**10.6**	**11.4**	**22.0**	*1943*	*86.7* [66.1]	1685 [1284]	**9.9**
6	Mar-79	23.9	**13.1**	**5.9**	**19.0**	**1793**	*66.7*	**1196**	**19.1**
7	Apr-79	18.9	**11.6**	**1.7**	**13..3**	*1642*	*69.4*	1140	**18.4**
8	May-79	15.1	*9.3*	0.0	*9.3*	*1305*	*63.8*	833	**4.4**
9	Jun-79	15.8	**8.9**	**0.8**	**9.7**	**1059**	**62.0**	**656**	**5.8**
10	Jul-79	13.8	*4.8*	0.48	5.3	*979*	*63.4*	621	1.3
11	Aug-79	14.7	*9.4*	0.0	*9.4*	**1259**	**63.4**	**798**	*2.6*
12	Sep-79	18.1	*13.8* [12.4]	1.4	13.8	*1910*	*56.2*	1073	*13.7*
13	Oct-79	20.4	*10.7* [13.2]	2.5	15.7	*1320* [1468]	*61.4*	**901**	*20.3*
14	Nov-79	24.4	*9.9* [13.1]	5.9 [6.6]	19.7	*2031*	*69.7*	1416	*6.3*
15	Dec-79	24.3	*9.2* [13.0]	6.5	19.5	*2224*	*46.7* [66.8]	**1485**	*6.9*
16	Jan-80	24.7	*12.9*	4.5 [7.2]	20.1	*2500*	**67.2**	**1681**	**17.0**
17	Feb-80	23.1	*12.3*	4.6	16.9	*1625*	*65.4*	1063	**20.6**
Maximum T		*28.0*	**7.1**	**16.7**	**23.8**	–	–	–	–

Table II. Note that decreases in viability are due to damage and bacterial degradation of detritus (Patrício & Marques, 2006).

2.2. *Statistical Analyses*

Statistical analyses were undertaken by Microsoft Excel, least squares regression using curvilinear polynomial types, including 2nd Order quadratic for one independent variable, such as water temperature and subsurface light intensity, compared with a given seagrass variable, such as *Zostera* growth rate, and linear and exponential for other relationships. The equations were evaluated on the basis of overall goodness of fit statistics using R^2 with p-value < 0.05 as acceptable. The effect of a water temperature increase due to recent climate change effects showed that the temperature increase of 1.4°C to 28°C on seagrass growth rates was consistent with the derived curvilinear water temperature equation using data from Holland (1982). The standard deviation, σ, for each point on the regression curve is shown using Excel Vertical Error Bars. The obtained significant R^2 values for higher-order curvilinear equations for the seasonal variation of water temperature and light intensity detected abnormal changes compared with the usual seasonal pattern. More complex statistical analyses were not expected to provide additional information for estuary managers to investigate variations in *Zostera* biomass and growth rate monitoring results.

The data sources from Holland (1982) used for analyses are shown in the data summary Table I, and could be found by clicking on the links below Table I and in the references and using the locations shown in the table. Hence, the actual data is also available by using the internet links shown below the summary table and in the references. To avoid confusion with reference to other data, the Holland (1982) sources are shown in italics with quotation marks.

Data gaps or limitations were investigated by having the data cross-checked for consistency between relationships with temperature and light conditions, and, where possible, with published data from other sources. In that regard, Ives *et al.* (2003) suggested that water temperature and light intensities be graphed and a curvilinear regression used to indicate significant variations and possible adjustment for consistency with the normal seasonal variation. For example, Plaisted *et al.* (2022, their Figure 4) showed *Zostera marina* abundance has a curvilinear relationship with water temperature, and Nielsen *et al.* (2002) found *Zostera marina* growth at depth depended on water turbidity. In addition, Jakeman *et al.* (2006) suggested consistency of the data be tested by an iterative process until convergence was obtained, so the various temperature relations were based on a reliable database. A similar iterative process was used for review of the more variable and difficult to measure light data under field conditions from Holland (1982). Note that in Section 3.2, it was noted that the *Zostera* biomass was lower at the low catchment population reference site than in the more highly populated areas of Lake Munmorah, indicating differences in sediment total phosphorus. Hence, no autocorrelation statistics, such as the Akaike information criterion (AIC), were required as no model selection was required. That is, it was likely that no spatial autocorrelation was present for the completely different sites. However, when comparing changes over time at the same reference site in Section 3.8, it was assumed that autocorrelation over time allowed estimation of unsampled months related to the measured values by

tracking the graph of changes over time. The adjusted values from these processes are shown in Table II. Estimated values for dates unable to be sampled are also shown, including estimated light intensities in the *Zostera* bed, loss rates, and gross growth rates, along with estimated biomass for months not sampled. Importantly, reference seagrass locations need to be used to provide a comparison with the selected routine sampling site. For example, broad-scale seagrass mapping by King and Holland (1986, see their Table I) for Zostera biomass in the Tuggerah Lakes coastal lagoon was undertaken using visually categorized percentage cover. The broad-scale sampling included the Munmorah Powered Station cooling water area in Budgewoi Lake, compared with reference areas Munmorah Lake and Tuggerah Lake. Recently, reference locations have been used to standardize the estimated seagrass biomass and areas during satellite image mapping in Southern Thailand (Koedsin *et al*., 2016).

3. Results

The summary Table III in the Discussion shows twelve equations were derived, which are important for seagrass estuary managers to understand because they are all interrelated. That is, each water temperature equation is connected in some way with all the others. Similar interrelated relationships exist for the light intensity equations, leading to catchment management of moderate levels of suspended sediment in runoff. The sediment total phosphorus relationship with biomass leads to a key understanding of catchment nutrient input controls on seagrass biomass stability over the long term.

3.1. Net Growth Rates with Water Temperature and Light Intensity

The data by Holland (1982) covered a range of temperatures from the minimum of 13.8°C in July 1979, to 26.6°C in March 1978, and a range of incident light intensities of 979 in July to 2500 µmol m^{-2} sec^{-1} in January 1980 (Table II). The range of *Zostera* net rates varied from 4.8 in July to 13.8 mg gdw^{-1} day^{-1} in September, 1979, with a 10-fold range in biomass from 2.6 in August, 1979, to 26.9 g dw m^{-2} in October, 1978. To test the consistency of the actual measured net growth rates (see *Table 6.1*) with temperature (*Appendix Al, page 194*), due to potential environmental changes during the 17 months of sampling were considered. A quadratic curvilinear 2nd Order relationship was derived for net growth rates with water temperature, as well as for Light intensities at 0.5 m inside the *Zostera capricorni* bed at the MF sampling site, using the data from Holland (1982), shown with some adjustments in the list in Table II. The water temperature relationship revealed the following net rate outliers relative to the others, which were investigated, and adjusted if necessary: a higher than expected 13.8 at 18.1°C in September, 1979, and lower than expected 10.7 mg gdw^{-1} day^{-1} in October, 1979, at the warmer 20.4°C. That also indicated the continuing decrease in net rates in November and December 1979 to 9.9 and 9.2 mg gdw^{-1} day^{-1}, while the temperatures increased to 24.4 and 24.3, respectively.

3.1.1. Summary of Data Processing for Adjustments and Estimation of Missing Results

The detailed data adjustment explanations in the Results Section are summarised in the notes to Table II. As the adjustments are important to obtaining reliable equations, the reasons for the adjustments are mentioned where necessary in the Results section.

Note to make the adjustments shown in the footnotes to Table II clearer, the font was increased, with the a), b), c) etc. relating to superscripts in the Table II column headings.

The light 2nd Order quadratic curve showed low net rates for November and December, 1979, with the water temperature data. It was also noted that the October 1979 net rate of 10.7 mg gdw^{-1} day^{-1} was not an outlier for the light intensity, indicating the light conditions in the *Zostera* bed modified the temperature-related net rate at the time of sampling. The incident intensities, I_0, in *Table 2*.2 show January 1979 as not sampled but were estimated from *Figure 2.7* in Holland (1982) at 2021 µmol m^{-2} sec^{-1}. The October, 1978 and January, 1979 incident light intensities in *Table 2.2* in Holland (1982) were unable to be measured and the March, June and August, 1979 measurements were indicated as low due to cloud cover or rain, so they were estimated by proportioning a measured intensity in µmol m^{-2} sec^{-1} with the Australian Bureau of Meteorology (BoM) light intensities at the nearby Norah Head Lighthouse (MJ m^{-2}) in 2022 for: January, 23.4, February, 19.0, March 14.0, April 12.9, May 10.196, June 10.4496, July 9.664, Aug 12.424, Sept 15.57, Oct 17.315. The estimated values are shown in Table II. To confirm that the BoM intensities give acceptable representations, they were tested by comparison with the measured values from 1978 to 1980 by a polynomial regression in Section 3.6.1, "Comparison of measured and estimated incident light intensities," and the results showed a reliable comparison.

Light intensities at 0.5m depth inside the *Zostera* bed, I_d, were calculated by multiplying incident light intensities in *Table 2.2* in Holland (1982) by percentage penetration of incident light in *Appendix Al, page* 196, e.g., $I_d = I_0 \times$ % penetration/100 µmol m^{-2} sec^{-1}. The percentage penetration value at 55% in August, 1979, was low due to cloud cover, and 46.7% in December, 1979, was lower than expected when tested with the relationship of I_d with I_0 by (9), below (I_d) = 0.7109 × incident light intensity (I_0) − 96.469 µmol m^{-2} sec^{-1}. The dates not able to be sampled were estimated by using the same equation. The January 1980 % penetration was not measured, and those not sampled were back calculated by 100 x I_d/I_0, with the I_d values. The estimated and adjusted % penetration is shown in Table II.

3.2. Zostera Biomass Relationship with Sediment Total Phosphorus

In the wider area of Lake Munmorah, where about half the nearshore catchment was highly urbanized, the *Zostera* leaf biomass at about 28 g dw m^{-2} (King & Hodgson, 1986 their Tables 3 and 4), was about double that at the MF site of about 12 g dw m^{-2}, indicating a higher nutrient input to the main body of the lake. As de Boer (2007)

indicated, moderate levels of sediment nutrients could promote seagrass growth; the total phosphorus (TP) content of seagrass bed sediments and its relationship with *Zostera* biomass were derived from the study by Harris (1977). Consequently, the stability of the *Zostera* leaf biomass at MF and in Lake Munmorah was compared in Section 3.8, and it was shown that the higher TP input maintained a higher and more stable biomass. The relative stability of the biomass indicated the importance of the three main environmental characteristics, and the detection of significant biomass changes over time could be used by estuary managers as part of their controls on catchment sediment and nutrient inputs.

The list of data adjustments and estimation of missing data is shown here. The a), b), c) etc. refer to the superscripts in the table headings.

a) Water temperatures in October 1978 and January 1979 from Holland (1982). Figure 2.4. Table 6.1 net rates had adjustments: September 1979 to 12.4 by 13.8 - 1.4 loss rate from 1.4 = (13.8 × [1 - 90 viability/100]) mg gdw^{-1} day^{-1} by viability of 90% estimated from Figure 6.2 for consistency with other net rates. October, 1979 10.7 to 13.2 = (10.7 + loss rate 2.5), see Section 3.2. November and December 1979 heatwave effects by net rate = gross rate - loss rate by (4) in Section 3.4, but the measured rates of 9.9 and 9.2 were consistent with the measured biomass in Table 5.2. November 1978 net rate at the highest measured water temperature of 26.6°C and potential maximum average daytime monthly average of 28°C, with Maximum T due to climate change 1.4°C added to 26.6°C, both estimated using (4). Not sampled and consistency with measured and adjusted estimated by $G_{gross} - L$.

b) Loss by net rate Table 5.1 × (1 - %viability/100) mg gdw^{-1} day^{-1} in Appendix A4. Loss rates adjusted consistently with Table 6.1 by: December 1978 adjusted from 5.1 to 4.1 by (3) November, 1979 5.9 to 6.6. July 1979 viability was shown as 90% in Figure 6.2 (down from 100% in Appendix A4), and the loss rate of 0.48 (4.8 × [1 - 90/100]) was consistent with a temperature of 13.8°C in Fig. 4. (3) indicated the loss rate in January, 1980 was about 7.2 at a temperature of 24.7°C rather than 4.5 (net rate 12.9 × [1 - 65%/100]), requiring a viability of 44%, giving 7.2 (12.9 × [1 - 44/100]) mg gdw-1 day–1. The not-sampled and November 1978, and maximum water temperature, 28°C, loss rates were estimated by (3).

c) Gross Growth Rates were estimated by measuring net rates in Table 6.1 plus L and not sampled by (2) derived from Fig. 3.

d) Incident light intensities, I0, are shown in Table 2.2 and the values affected by cloud or rain in March, June and August, 1979, and the unable to sample October, 1978 and January, 1979, were estimated by proportioning with the Australian Bureau of Meteorology (BoM) average monthly light intensities at the nearby Norah Head Lighthouse. In addition, the October 1979 value of 1320 was low compared to other intensities, so it was adjusted to 1468 by (1320 μmol m^{-2} sec^{-1} × October MJ m-2 17.315/September 15.57). The adjusted values were consistent with Fig. 9 and derived (9) light intensities inside the Zostera bed with incident light intensities.

e) The not sampled % Light intensity reaching 0.5m inside the Zostera bed was back calculated from the 100 x Id/I0, where Id is the estimated bed light intensity and I0 is the incident intensity. In February 1979, the % was adjusted from 86.7 to 66.1.

f) Light intensities reaching 0.5m inside the Zostera bed, Id, were estimated by Id = I0 × % light penetration/100, using incident light intensities in Table 2.2 and % light penetration in Appendix Al, page 196. Not sampled ID estimated by (9).

g) Measured biomass is in Holland (1982) *Table 5.2*. The not sampled *Zostera* biomass, g dw m^{-2}, values were estimated by (11): B = 4.0106 x G_{net} − 32.885 relationship of biomass in *Table 5.2* with the measured net growth rates in *Table 6.1*. October 1978 biomass of 26.9 was adjusted for consistency with the measured net rate of 12.8 mg gdw^{-1} day^{-1} to 18.5 gdw m^{-2} by (11). The July 1979 biomass was estimated by proportioning the August biomass, 2.6 g dw m$^{-2,}$ by the July and August net rates, giving 1.3 g dw m^{-2} (2.6 × 4.8/9.4).

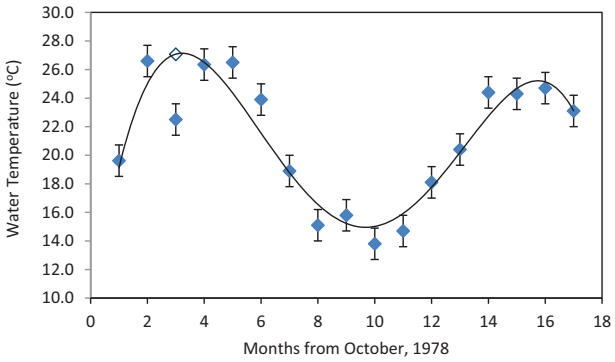

Fig. 1. Monthly water temperature variations at the Lake Munmorah *Zostera* bed sampling site from October 1978 to February 1980 (redrawn from *Figure 2.4* "*Seasonal variation in water temperature at four field sites in Lakes Munmorah and Budgewoi. Munmorah Flats*." The water temperatures in October 1978 at 19.6°C and January 1979 of 26.3°C were estimated from the same Figure. As the water temperature of 22.5°C in December 1978 was lower than expected, the temperature of 27.1°C (open blue diamond) was estimated using the regression equation, but not included in the regression. Error bars are the standard deviation ($\sigma \pm 1.11$) of absolute differences between each reported and estimated temperature.).

3.3. Seasonal Variation in Water Temperatures

The seasonal water temperature variation derived from raw data in *Figure 2.4* in Holland (1982) is shown in Fig. 1. Although seasonal water temperature variations are usually assumed to vary as a sine curve (Saborowski & Hünerlage, 2022), it is unlikely the summer and winter conditions are the same each year, so the temperature variations were assumed to be describe by a curvilinear relationship.

The curvilinear relationship in Fig. 1 was obtained using the 4th-order polynomial:

$$\text{Water temperature} = -0.0073 \times (\text{month since October, 1978})^4 + 0.2778 \times (\text{month since} = \text{October, 1978})^3$$

$$- 3.4095 \times (\text{month since October, 1978})^2 + 14.289 \times (\text{month since October, 1978}) + 7.9803 \quad (1)$$

with $R^2 = 0.8634$, n = 17, p > 0.001. Note (month since October 1978)^n is calculated by POWER (number, n). The low temperature in December 1978 was investigated by examining the relationship between gross, loss, and net rates with temperature in Figs. 3 and 4, which showed the measured temperature was consistent, indicating an abnormally low temperature at the time of measuring the net growth rate of 12.8 mg gdw^{-1} day^{-1}.

3.4. *Seasonal Variation in Net Growth Rates*

Due to environmental variations and difficult field measurements, the net growth rates showed variations in September, October, November, and December 1979 from the theoretical quadratic curve with water temperature. The September 1979 net rate of 13.8 was adjusted to 12.4 by subtracting the loss rate estimated as 1.4 (13.8 × [1 − 90/100]) mg$^-$ gdw^{-1} day^{-1} by an estimated viability of 90%, giving a consistent loss rate with water temperature in Fig. 4. In October, 1979, the loss rate of 2.5 (10.7 × [1 − viability 77/100]) in *Appendix A4*: "*Percentage Viability Lake Budgewoi Test Sites"* was consistent with the water temperature/loss rate relationship in Fig. 4, but the net rate of 10.7 appeared low for a temperature of 20.4°C, suggesting a net rate of 13.2 (10.7 + 2.5) mg gdw^{-1} day^{-1}. That was tested by the relationship of gross growth rate with water temperature in Fig. 3. The probable gross rate of 15.7 (net 13.2 + 2.5 loss rate) mg gdw^{-1} day^{-1}plotted against water temperature was consistent with the regression obtained by (2). The adjusted net rates are shown in Table II.

As the growth rates during the southern spring/summer of November and December 1979 of 9.9 and 9.2 mg gdw^{-1} day^{-1} were much lower than over the same period in 1978, the cause was investigated. It was noted that a heatwave event occurred on those dates, causing the *Zostera* bed water temperatures to reach 28.7°C and 29.5°C, respectively (page 24 in Holland, 1982), probably suppressing the growth rate measurements. The reported net rates were measured at lower temperatures of 24.4°C and 24.3 °C, apparently after the heatwave had finished. However, it

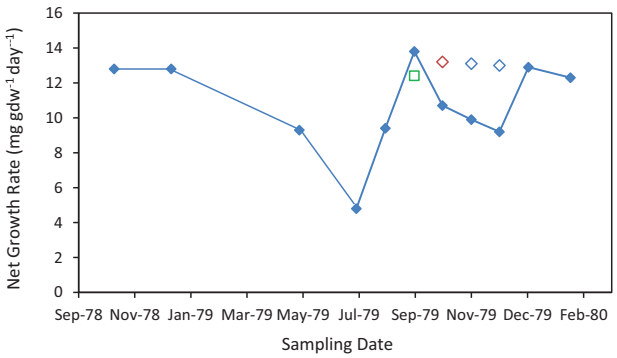

Fig. 2. Seasonal variation of *Zostera* net growth rate (redrawn from Holland (1982) *Figure 6.3* "*Comparative growth rates of Zostera capricorni at the four field sites at Munmorah Flats*". Adjustments are shown in Table II for September 1979 by subtracting loss rate 1.4 (open green square), October 1979 by adding loss rate 2.5 (open red diamond), and due to heatwave effects in November and December 1979 (open blue diamonds).

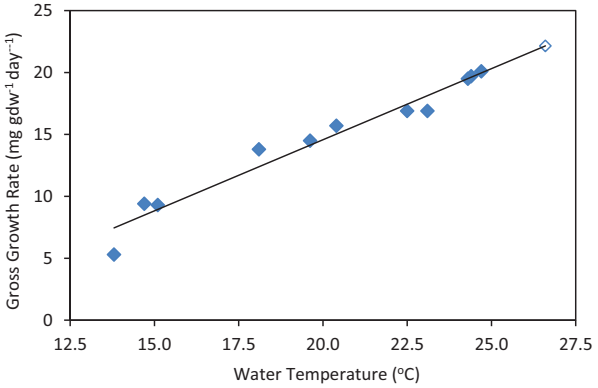

Fig. 3. Relationship of *Zostera* Gross growth rate with water temperatures (from Gross rates in Table II and temperatures *from Appendix Al* in Holland (1982). The adjusted gross rates for October 1979, at 20.4°C of 15.7 mg gdw^{-1} day^{-1}and November and December 1979, at 24.4°C and 24.3°C of 19.7 and 19.5 mg gdw^{-1} day^{-1}, respectively, from Table II were included in the regression. The estimated gross rate of 22.1 mg gdw^{-1} day^{-1} (open blue diamond) at the highest measured temperature of 26.6°C was not part of the regression.

appears the plants had been damaged in some way by the heatwave, so the expected rates were estimated from the relationship of gross rates with temperature; see Fig. 3, minus the estimated and adjusted loss rates in Table II, giving the adjusted net rates of 13.1 and 13.0 mg gdw^{-1} day^{-1}, respectively, which are also shown in Table II. The seasonal variation in net growth rate is shown in Fig. 2 from *Figure 6.3:* in Holland (1982), with adjustments for effects of water temperature variations, potential light intensity effects, and loss rates.

3.5. *Relationships of Gross, Loss, and Net Growth Rates with Water Temperature*

The study by Santamaría and van Vierssen (1997) showed that water temperature governed the *Zostera* biological processes, and the more variable light conditions modified the response to water temperature, so water temperature was examined first. As the gross growth rates are estimated from G_{net} + L in Table II, the gross growth rates are compared with water temperatures from *Appendix Al* (Holland, 1982) in Fig. 3.

The relationship obtained in Fig. 3 was:

$$\text{Gross growth rate } \left(\text{mg gdw}^{-1}\text{day}^{-1}\right) = 1.148 \times \text{Water temperature } (^\circ C) - 8.3893 \quad (2)$$

$R^2 = 0.9573$, n = 11, p > 0.001. To complete the representation, the loss rate relationship with water temperature is shown in Fig. 4.

The relationship obtained in Fig. 4 is given by:

$$\text{Loss Rate } \left(\text{mg gdw}^{-1}\text{day}^{--1}\right) = 0.0143 \times e^{(0.2522 \times T)} \quad (3)$$

with $R^2 = 0.9889$, n = 9, p > 0.001. As the net rate could be estimated by the difference between gross growth rates by (2), minus the loss rate, L, by (3), the net growth rate could be estimated by:

$$\text{Net growth rate} = 1.148 \times \text{T} - 8.3893 - 0.0143 \times e^{(0.2522 \times \text{T})} \quad (4)$$

3.5.1. Relationship of Net Growth Rate with Water Temperature

The quadratic relationship of net growth rate with water temperature is shown in Fig. 5, using the measured net growth rates in Fig. 2 with the October, November, and December 1979 adjustments. To provide a more detailed understanding of the relationship, the estimated net rate of 10.4 mg gdw^{-1} day^{-1}at the highest measured temperature of 26.6°C in November 1978 by (4) was also included. As water temperatures are likely to increase in coastal lagoons with climate change, the maximum average day-time water temperature in the hottest summer month increased by 1.4°C, as indicated by the overall lagoon increase by Scanes *et al*. (2020). That gave a water temperature increase to 28.0°C, giving an estimated net rate of 7.1 mg gdw^{-1} day^{-1} from Table II. The curve allowed estimation of the optimum temperature and the maximum net growth rate.

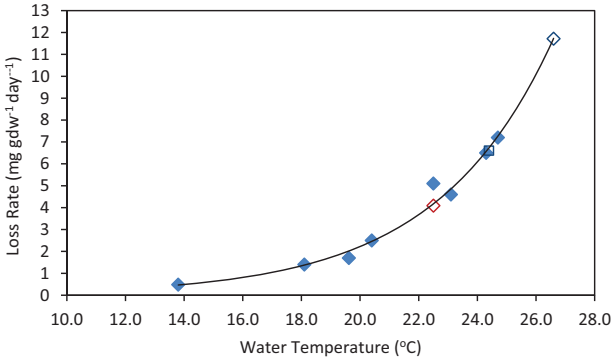

Fig. 4. Relationship of *Zostera* loss rate with water temperature (estimated and adjusted loss rates are from Table II, and water temperatures in *Appendix Al* in Holland (1982). The November 1979 rate at 24.4°C of 5.9 was adjusted to 6.6 (open blue square), for consistency with the gross rate and estimated net rate of 13.1 mg gdw^{-1} day^{-1} in Table II. The lowest loss rate at 13.8°C in July 1979 was adjusted from zero to 0.48 based on 90% viability in *Figure 6.2*. Note the measured loss rate of 5.1 in December 1978, with a low temperature 22.5°C was higher than expected, so the regression was used to estimate the likely rate of 4.1 mg gdw^{-1} day^{-1} (open red diamond) but not used in the regression. The highest estimated loss rate of 11.7 mg gdw^{-1} day^{-1}at the highest water temperature recorded of 26.6°C in November 1978 (open blue diamond) was also not used in the regression. The May and August 1979 zero loss rates (100% viability in *Appendix A4*) were not included because they are not recognized by an exponential equation.

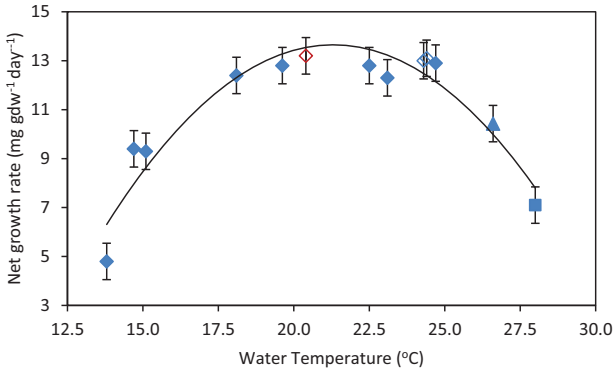

Fig. 5. Quadratic 2nd Order relationship of net growth rate of *Zostera* with water temperatures. (net growth rates for October 13.2 mg gdw^{-1} day^{-1} (open red diamond) and November and December, 1979 heatwave adjusted 13.1 and 13.0 mg gdw^{-1} day^{-1} (open blue diamonds) as described in Fig. 2) Due to high correlations of the gross and loss rates, above, the net rate of 10.4 mg gdw^{-1} day^{-1}at 26.6°C (blue triangle) and the expected maximum average day-time water temperature of 28.0°C with estimated net rate of 7.1 mg gdw^{-1} day^{-1} (blue square) are also included. Net growth rate error bars 2σ ± 0.82.

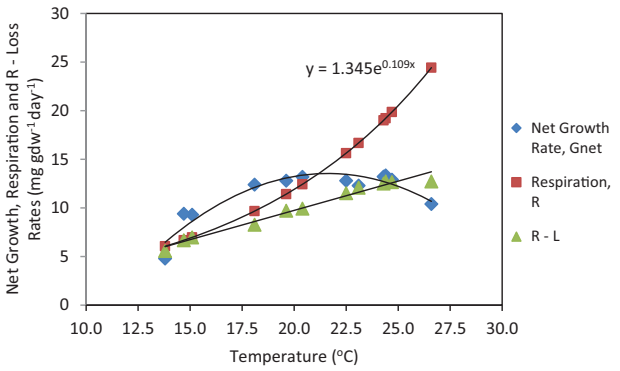

Fig. 6. Respiration rate at the average optimum temperature for *Zostera capricorni*. Comparisons are shown with the estimated respiration rate, R, with the quadratic net growth rate, G_{net}, to the highest temperature recorded in the seagrass bed of 26.6°C, and the difference between respiration, R, and loss rates, L. The resulting equations are R - L = 0.6017 × T −2.2865 (R^2 = 0.9767, n = 12, P > 0.001) and G_{net} = −0.1157 × T^2 + 5.0033 × T −40.543 (R^2 = 0.8904, n = 12, p > 0.001).

The quadratic 2nd Order polynomial relationship obtained is:

$$\text{Net Growth Rate}\left(\text{mg gdw}^{-1}\text{day}^{--1}\right) = -0.1305 \times T^2 + 5.5604 \times T - 45.569 \quad (5)$$

with R^2 = 0.9024, n = 13, p > 0.001. Importantly, there was a reduction in growth rate by about 32% by the expected 1.4°C water temperature increase by climate change from 10.43 mg gdw^{-1} day^{-1} at 26.6°C in November 1978 (Table I) to 7.1 mg gdw^{-1} day^{-1} at 28°C. This demonstrates how the quadratic curvilinear relationship could indicate adverse impacts on seagrass due to water temperature increases by processes such as climate change and leading to a need for appropriate mitigation measures.

The optimum temperature, T_{opt}, was estimated in Fig. 5 at 21.3 ± 1.05°C, and the maximum net growth rate production was 13.7 ± 0.55 mg gdw^{-1} day^{-1}. By comparison, T_{opt} is about 11.6% lower than 24.1°C estimated for the subspecies *Zostera muelleri* by Collier *et al*. (2017), which is consistent with the error bars in Fig. 5 showing there is little practical difference between the results.

Note that it is not feasible to extend the curve in Fig. 5 to higher temperatures than 28°C because thermal effects begin to occur, which do not follow the biological processes occurring in the normal temperature range averaged over a daytime monthly period. For example, thermal effects on seagrass growth rates are time and temperature-dependent, as shown by Holland (1982). At 29°C, the growth rate decreased by 29% after 24 hours and 36.2% at 48 hours. Importantly, after 96 hours, the *Zostera* began to acclimate to the high temperatures with a lower reduction of 15.9% and at 31°C, compared to the control at 27°C with a net rate of 6.9 mg$^{-gdw\text{-}day}$. Those results are related to thermal tolerance, which is measured as LD50, meaning

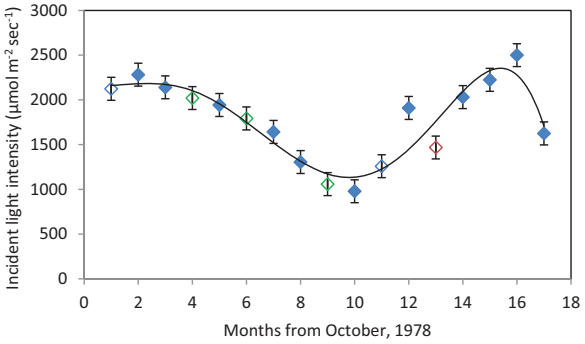

Fig. 7. Seasonal variation of incident light intensities at the Lake Munmorah sampling site modified from *Figure 2.8* "*Temperature, salinity and incident light data for Lake Munmorah*" in (Holland, 1982). The estimated values for October, 1978 at 2124 and August, 1979 at 1259 (open blue diamonds) and adjustments in October, 1979 of 1468 µmol m^{-2} sec^{-1} (open red diamond) are shown, including the January, March and June, 1979 estimated intensities not associated with measured net rates (open green diamonds), with values 2021, 1793 and 1059 µmol m^{-2} sec^{-1}, respectively. Error bars are $\sigma \pm$ 128 µmol m^{-2} sec^{-1} of absolute difference between measured and estimated light intensities.

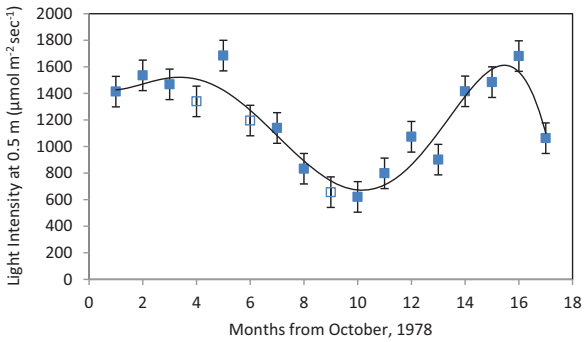

Fig. 8. Seasonal variation light intensities at 0.5m inside the *Zostera* bed at the Lake Munmorah sampling site from October, 1978. Derived from incident light intensities in *Table 2.2*, multiplied by light penetration from *Appendix A1*, page 196 in Holland (1982), with additions and adjustments. The values in open squares are estimates not related to measured net rates. Error bars are $2\sigma \pm$ 115 (µmol m^{-2} sec^{-1}) of absolute differences between measured and estimated light intensities.

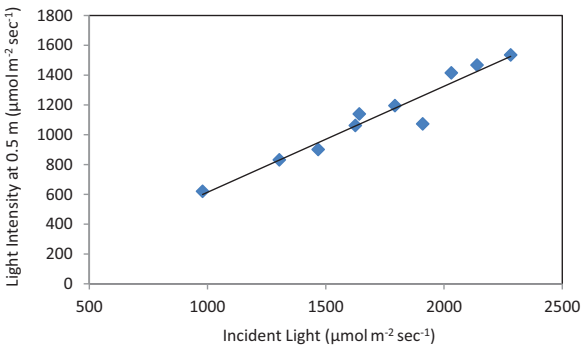

Fig. 9. Relationship of light intensities at 0.5 m (I_d) inside the *Zostera* bed. Derived from the incident light intensities (I_0) in *Table 2.2* with measured percent penetration in *Appendix A1* in Holland (1982), including estimated I_0 for March and October, 1979 in Table II.

the lethal temperature causing 50% mortality, typically for an exposure time of 96 hours (ASTM E729-96, 2014). By comparing the reductions in viability in *Table 6.5* "*Viability*

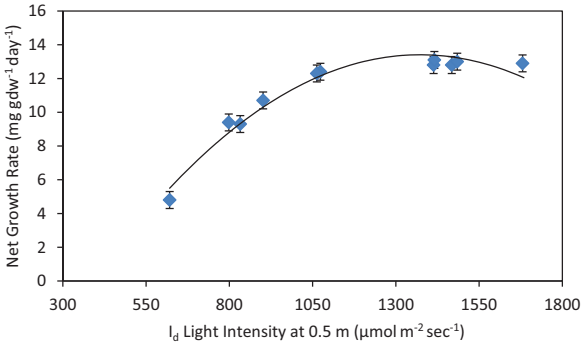

Fig. 10. Quadratic 2nd Order relationship of net growth rate with light intensity at I_d 0.5 m depth in the *Zostera* bed. The relationship was obtained using the measured rates in *Table 6.1* and adjusted rates for September 1979 and heatwave affected in Table II, while October 1979 was the same as measured in *Table 6.1* at 10.7 mg gdw^{-1} day^{-1} at light intensity 901 µmol m^{-2} sec^{-1} in Table II. Error bars are $2\sigma \pm 0.50$.

of Zostera shoots after a range of exposure times" in Holland (1982), with the 96-hour acclimatized growth rates, the estimated LD50 was about 32°C. Additionally, climate change could cause seagrass biomass and growth rates to decrease with an increase in summer water temperatures > 28°C (see Shields *et al*., 2018), a similar climate change effect as shown in Fig. 5 and is worthy of further research for carbon emission mitigation.

3.5.2. *Respiration Rate at the Optimum Temperature*

Although the leaf marking method takes into account the leaf loss rate, the plant is still respiring, so the effect of the respiration rate on the net rate was investigated. Theoretically, the respiration rate, R, equals the maximum net rate at the optimum temperature. That was tested by setting R equal to the water temperature related G_{net} of 13.7 mg gdw^{-1} day^{-1} at T_{opt} of 21.3°C. It was assumed that the difference between R and the estimated and adjusted loss rates, L, in Table II was expected to give similar net rates as measured in *Table 6.1* with the Table II adjustments, including G_{net} of 10.4 mg gdw^{-1} day^{-1} with temperature to the measured highest temperature of 26.6°C. The relationship of respiration rate with net growth rate, compared with the quadratic net growth rate and R-L, is shown in Fig. 6.

The respiration rate at the average optimum temperature of 21.3°C, corresponding with the maximum net rate of 13.6 mg gdw^{-1} day^{-1}, estimated from Fig. 6, was given by the exponential equation:

$$\text{Respiration rate}\left(\text{mg gdw}^{-1}\text{day}^{-1}\right) = 1.345 \times e^{(0.109 \times T)} \quad (6)$$

Although the R-L regression estimated the lowest net rate at 5.6, similar to the lowest G_{net} of 4.8 $mg^{-gdw\text{-}day}$ at the lowest water temperature of 13.8°C, it overestimated the net rate as 12.7 at the highest temperature of 26.6°C in November 1978, compared to 10.4 mg gdw^{-1} day^{-1} in Table II. Those observations show the steeper loss rate relationship with water temperature in Fig. 4 overrides the effects of respiration rate, indicating the appropriate leaf marking method for use of loss rates to estimate net rates, as suggested by Holland (1982).

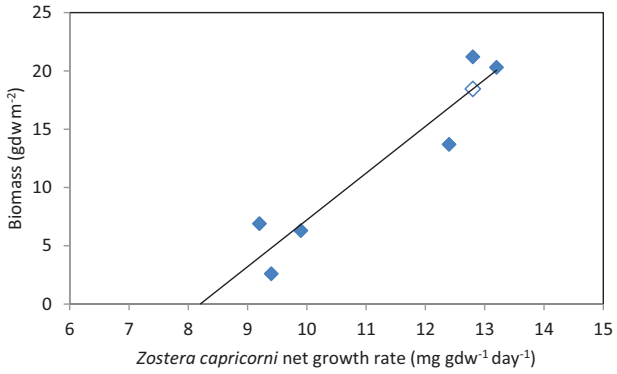

Fig. 11. Relationship of *Zostera* biomass with net growth rates (from *Table 5.2* and *Table 6.1* in Holland, 1982). Derived using the September and October, 1979 adjusted rates of 12.4 and 13.2 mg gdw^{-1} day^{-1}, respectively, in Table II, while the measured heatwave November and December, 1979 rates of 9.9 and 9.2 mg gdw^{-1} day^{-1} are consistent with the biomass measurements. The October, 1978 biomass was adjusted from 26.9 to 18.5 g dw m^{-2} in Table II using the measured net rate of 12.8 mg gdw^{-1} day^{-1} by the regression equation (open diamond), but not used in the regression.

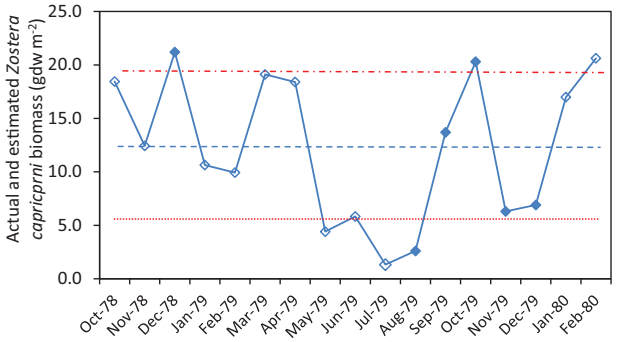

Fig. 12. Stability Chart of seasonal variation of *Zostera* biomass (g dw m^{-2}) at site MF. (From *Table 5.2* in (Holland, 1982) with estimated and adjusted (open diamonds) in Table II by (11)). That gave an average of 12.3 (blue dashed line) and a standard deviation of 6.8, with upper 19.1 (red dotted line) and lower investigation level (red dotted line) of 5.5 g dw m^{-2} by average ± 1σ.

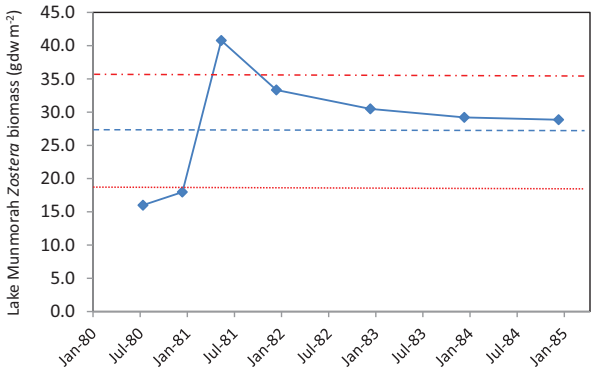

Fig. 13. Stability Chart of long-term changes of *Zostera* biomass (g dw m^{-2}) in the whole of Lake Munmorah. (From August 1980 to January/February 1985, calculated as biomass (tonne) from Table IV divided by area (Km^2) in Table III from King and Hodgson (1986)). That gave a Stability Chart average of 28.1 with upper 36.7 and lower investigation level of 19.5 g dw m^{-2} by average ± 1σ = 8.6.

3.6. Relationships of Net Growth Rates with Light Intensities Inside the Zostera Bed Derived from Incident Light Intensities

Due to difficulties with field measurements, two of the 11 incident light intensity measurements, corresponding with G_{net} in October 1978 and August 1979, could not able to be measured, so they were estimated using the local BoM measurements at the Norah Head Lighthouse in 2022, with details of those estimates shown in the footnotes to Table II.

3.6.1. Comparison of Measured and Estimated Incident Light Intensities

To confirm the BoM values were suitable to estimate unmeasured or make adjustments for the period of sampling, Fig. 7 shows a comparison of the season variation in BoM estimated and measured incident light intensities. The seasonal variation from October 1978 to February 1980 was estimated by a 5th-order polynomial regression.

The curvilinear relationship obtained in Fig. 7 indicated that the BoM incident light intensities gave a reasonable comparison with the measured and adjusted values by:

$$\begin{aligned}\text{Incident light intensities } (\mu\ \text{molm}^{-2}\text{sec}^{-1}) \\ = -0.0694 \times (\text{month since October, 1978})^5 \\ + 2.4777 \times (\text{month since October, 1978})^4 \\ - 27.509 \times (\text{month since October, 1978})^3 \\ + 97.822 \times (\text{month since October, 1978})^2 \\ - 117.98 \times (\text{month since October, 1978}) + 2206.8 \quad (7)\end{aligned}$$

with $R^2 = 0.8601$, n = 17, $p > 0.001$.

The exception was the light intensity of 1910 µmol m^{-2} sec^{-1} in September 1979 (month 12), which was higher than expected for that month. The increase was investigated in relation to the known 11-year solar cycle reported by Fickling and Dougherty (1983). They noted a large increase in the 1979 solar cycle activity index in both the northern and southern hemispheres, with a maximum in October at 11.4 and a similar 10.1 in September 1979, so the 1910 µmol m^{-2} sec^{-1} was used to estimate light intensities inside the *Zostera* bed. In addition, Fickling and Dougherty (1983) noted the 11 year solar activity in 1978 was higher than in 1979, supported by a solar storm in November, 1978 (Cane & Richardson, 1997), so the unmeasured light intensity in October, 1978 was estimated at 2124 (Sept-79 1910 µmol m^{-2} sec^{-1} × BoM MJ^{-m2} in October 17.315/September 15.57) µmol m^{-2} sec^{-1}, which was consistent with the seasonal comparison in Fig. 7. In addition, the I_0 measurements in October 1979 of 1320 appeared low, so it was also investigated. As it was associated with a solar maximum event, the value of 1320 was adjusted using the relevant BoM intensities to 1468 (1320 × October 17.315/September 15.57) µmol m^{-2} sec^{-1}.

3.6.2. Seasonal Variation of Light Intensities Inside the Zostera Bed

The seasonal variation of light intensities at 0.5m inside the *Zostera* bed, I_d, was estimated by multiplying the incident intensities, I_0, from *Table 2.2* by the % light penetration from Appendix Al, page 196, and January 1980

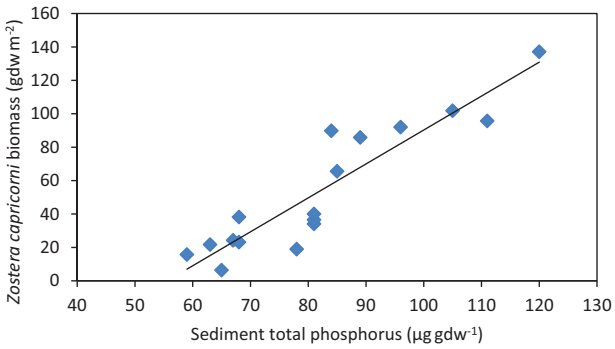

Fig. 14. *Zostera* biomass relationship with sediment total phosphorus in Lake Illawarra. (From data in (Harris, 1977) in the nearby Lake Illawarra).

at 80% from *Figure 2.7* in Holland (1982). The results are shown in Table II. It was assumed the light conditions would relate to the above temperature-related net growth rates, while the light conditions may also reveal effects of the local water turbidity conditions in the *Zostera* bed. The following estimates or adjustments to the *Zostera* bed I_d were estimated or made by proportioning with the BoM measurements and are shown in Table II. The I_d values in October 1978, August, and December 1979, and January 1980 were estimated from the regression shown in Fig. 9, and percentages by back calculation. October 1978 was estimated from I_0 of 2124 by (9) as 1421 µmol m^{-2} sec^{-1}, giving % penetration of 66.9 (100 × 1421/2124), similar to the measured average of 64.6%. In August 1979, I_d was also estimated from I_0 of 1259 as 798 µmol m^{-2} sec^{-1}, giving % penetration 63.4. In December 1979, by I_0 2224 to I_d 1485, gave % penetration 66.8, and in January 1980, I_0 2500 to I_d 1681, % penetration 67.2. The measured October 1979 I_0 of 1320 appeared low, being similar to the May 1979 value 1304, so it was adjusted to 1468 µmol m^{-2} sec^{-1} by the BoM values for October and September (1320 × 17.315/15.57). By applying the measured 61.4% penetration, the I_d value was estimated at 901 µmol m^{-2} sec^{-1}, which is also shown in Table II. Fig. 8 shows the seasonal variation of estimated light intensities at 0.5m inside the *Zostera* bed.

The curvilinear relationship obtained in Fig. 8 was the 5th-order polynomial:

$$\begin{aligned}&\text{Light intensities at 0.5 m inside the Zosterai bed}\\&= -0.0667 \times (\text{month since October, 1978})^5\\&\quad + 2.4894 \times (\text{month since October, 1978})^4\\&\quad - 29.877 \times (\text{month since October, 1978})^3\\&\quad + 123.68 \times (\text{month since October, 1978})^2\\&\quad - 152.76 \times (\text{month since October, 1978})\\&\quad + 1482.8 \qquad (8)\end{aligned}$$

with $R^2 = 0.8707$, n = 17, p > 0.001.

Although the February 1979 incident light intensity of 1943 was consistent with the seasonal variation in Fig. 7, the *Zostera* bed I_d of 1625 µmol m^{-2} sec^{-1} was shown as high in Fig. 9 compared to other values, so the cause was investigated. (9) estimated the I_d at 1284 µmol m^{-2} sec^{-1}. However, the February 1979 value was not related to a measured net growth rate, so it had no effect on the relationship of net rate with I_d in Fig. 10.

3.6.3. Relationship of Light Intensities Inside the Zostera Bed with Incident Light Intensities

As shown above, the amount of light reaching 0.5 m inside the *Zostera* bed was unknown for some dates, so the relationship of I_d with I_0 for measured % penetration measurements was estimated, and the relationship is shown in Fig. 9.

The regression obtained in Fig. 9 was:

$$\begin{aligned}&\text{Light intensity at 0.5 m}(I_d)\\&= 0.7109 \times \text{incident light intensity } (I_0) - 96.469 \qquad (9)\end{aligned}$$

with $R^2 = 0.9359$, n = 10, p > 0.001.

As the relationship of light intensities in the *Zostera* bed was confirmed as directly related to the incident intensities, the relationship of I_d with net growth rates was examined.

3.6.4. Relationships of Net Growth Rates with Light Intensities Inside the Zostera Bed

Although the literature indicated a relationship of net growth rate with light intensity inside the *Zostera capricorni* bed to be asymptotic, with photo-inhibition at high intensities measured in *Table 6.1* in Holland (1982), and with the adjusted rates for September, November, and December, 1979, from Table II, a quadratic relationship was derived in Fig. 10.

The quadratic relationship in Fig. 10 is given by:

$$\begin{aligned}&\text{Net Growth Rate (mg gdw}^{-1}\text{day}^{-1})\\&= -1.40\text{E}-05 \times I_d^2 + 0.0384 \times I_d - 12.944 \qquad (10)\end{aligned}$$

for $R^2 = 0.9617$, n = 11, p > 0.001 where I_d is Light Intensity (µmol m^{-2} sec^{-1}) at 0.5 m in the *Zostera* bed.

The maximum G_{net} of 13.4 ± 0.25 mg gdw^{-1} day^{-1} was about 9.5% lower than the northern summer June and August average of 14.8 for *Zostera marina* by Dennison and Alberte, (1985, their Table 3), converted from their average of 4.9 mg C gdw^{-1} day^{-1} to 14.8 = (4.9/0.33) mg gdw^{-1} day^{-1} using the average carbon content of 33% by Duarte (1990, see Figure. 2). Light intensity before photo-inhibition was estimated as 1370 ± 45 µmol m^{-2} sec^{-1}. Note that the unadjusted October 1979 rate of 10.7 mg gdw^{-1} day^{-1} in Table II indicates that the *Zostera* bed light intensities limited the water temperature-related net rate of 13.2 mg gdw^{-1} day^{-1}, but not the other measured or adjusted rates.

The light intensity maximum G_{net} was similar to the water temperature value of 13.7, because the seasonal light intensity drives both the water temperature and *Zostera* photosynthesis, as found by Cabello-Pasini *et al.* (2003) for *Zostera marina*. In addition, although Figs. 5 and 10 may provide estuary managers with insights into how water temperatures and light intensity conditions affect *Zostera* production, Lee *et al.* (2007) showed sediment nutrient concentrations, particularly phosphorus from land eroded soils, could also have a significant effect on growth rates,

production, and biomass. Hence, the effect of phosphorus on *Zostera* net growth rates was investigated, but first it was necessary to determine the relationship of *Zostera* biomass in Lake Munmorah with the above net rates.

3.7. *Relationship of Biomass with Net Growth Rates*

The biomass of *Zostera* was estimated by Holland (1982) in *Table 5. "Zostera reproductive shoots shoot weight, frequency and biomass*." by multiplying the mean shoot weight (mg dw shoot^{-1}) by the shoot frequency (g dw m^{-2}). The *Zostera* biomass was assumed to be related to the net growth rate, so it was investigated in Fig. 11.

The relationship from Fig. 11 is given by:

$$\text{Zostera capricorni biomass } (\text{gdw m}^{-2}) = 4.0106 \times \text{Net growth rate } \left(\text{mgdw gdw}^{-1}\text{day}^{-1}\right) - 32.885 \quad (11)$$

with $R^2 = 0.8976$, n = 6, $p > 0.01$. The regression indicated *Zostera* biomass to become nil at G_{net} of 8.2 mg gdw^{-1} day^{-1}, which was likely to occur during the southern winter conditions of low light and temperatures, measured in July 1979 at 979 µmol m^{-2} sec^{-1} and the temperature of 13.8°C. However, the measured biomass in August 1979 was unexpectedly low at 2.6 g dw m^{-2}, which appears due to the likely low nutrient catchment inputs to the sampling site. The maximum G_{net} of 13.4 mg g dw^{-1} day^{-1}, see Fig. 10, was estimated to produce a biomass of 20.9 g dw m^{-2} using (11). That was investigated by the seasonal trend at the MF sampling site, compared to the long−term biomass changes in the whole of Lake Munmorah using Stability Charts.

3.8. *Stability of Zostera Biomass Long-Term Changes*

The stability of a freshwater aquatic ecosystem was investigated by Ives *et al*. (2003), who found the system was stable when the variability of the long-term abundance was less than the variability of the environmental factors such as temperature, nutrient inputs, or other factors causing the system's abundance to change. Hence, Stability Charts for the seasonal variation of *Zostera* biomass with upper and lower standard deviations from the long-term average (derived from the study by Carr *et al*., 2012) are used here to show *Zostera* biomass changes. The stability Chart helps to identify responses to temperature and light conditions, along with catchment nutrient inputs. As the relationships obtained are reasonably consistent, the seasonal changes in *Zostera* biomass at the MF site from *Table 5.2* in Holland (1982), including the estimated not-sampled months in Table II using (11), were tracked by a graph of changes over time. The missing biomass values in Fig. 12 were estimated from the regression in Fig. 11, which has a standard deviation for differences between each reported and estimated biomass value of $\sigma \pm 1.65$, giving confidence about 13% of the average biomass of 12.3 g dw m^{-2}. That gave a realistic estimate of the missing biomass.

The Stability Chart shows changes that may require further investigation of potentially unknown environmental effects. For example, Hodgson and Bucher (2023) showed the long-term changes for average total seagrass area ± 1 standard deviation, σ, in coastal lagoons gave a reasonable estimate of the variability. They found in Lake Macquarie, 1σ accounted for about 85% of the long-term variability. Hence, it was assumed the seasonal *Zostera* biomass changes at MF could also be compared to the average ± 1σ, which is shown in Fig. 12 Stability Chart for biomass changes.

The Stability Chart accounted for 70.6% of the observations with a wide range about the average of 12.3 from 2.6 to 21.2 g dw m^{-2} around the average. In addition, the above estimated biomass of 20.9 g dw m^{-2} for maximum G_{net} 13.4 mg gdw^{-1} day^{-1} was almost the same as the upper biomass range, indicating consistency of the light intensity-derived net rate with biomass. However, the chart shows biomass was related to the heatwave-affected net rates of 9.9 and 9.2 in November and December 1979, whereas Fig. 5 shows the higher adjusted net rates of 13.1 and 13.0 mg gdw^{-1} day^{-1} in Table II were related to water temperature. That finding is supported by those of George *et al*. (2018) that high water temperatures have a greater effect on biomass than photosynthesis. Fig. 12 also shows the southern autumn and winter, May to August, 1979, levels at or below the lower investigation level. The cause was investigated by examining the August 1980 seagrass map (see Figure 4 in King & Holland, 1986), which shows that nearly all the MF sampling sites used by Holland (1982) were covered with a high abundance of *Ruppia* and no *Zostera* in the area covered by the *Ruppia*. Catchment nutrient inputs were observed by Cho *et al*. (2009), causing an increased abundance of *Ruppia maritima*, the same species that occurs in the Tuggerah Lakes (King & Holland, 1986). However, Holland (1982) did not find excessive *Ruppia* or macroalgae at the MF site. That indicates a change in environmental conditions in August 1980, so the change was investigated by a Stability Chart of the long-term changes in *Zostera* biomass for the whole of Lake Munmorah by King and Hodgson (1986), which is highly urbanized in the southern half, shown here in Fig. 13.

The Fig. 13 shows that the whole lake chart accounted for 82% of the variability, with a range about the average of 28.1 from 16 to 40.8 g dw m^{-2}. The lowest biomass of 16.0 in August 1980, was about 13-fold higher than the 2.6 g dw m^{-2} in August 1979, at the MF site, while the whole lake average was about twice that at the MF site, with the highest at 40.8 g dw m^{-2} during southern winter, June 1981. Those observations indicate that the higher biomass and lower variability than at MF could be due to nutrient inputs from the more densely urbanized nearshore catchment in the southern areas of Lake Munmorah. Consequently, the estimated MF site biomass of 20.9 g dw m^{-2}; for maximum G_{net} of 13.4 mg$^{-\text{gdw−day}}$ was now near the lower biomass range for Lake Munmorah. That suggests, for the maximum G_{net} to be related to the upper biomass in Lake Munmorah of 36.7 g dw m^{-2}, the whole of Fig. 10 quadratic relationship may have to be increased to give a higher maximum G_{net} in the lake of about 17.4 (36.7 + 32.885/4.0106) mg gdw^{-1} day^{-1} by (11). Hence, the potential G_{net} increase by sediment TP concentrations was tested by examining the relationship of *Zostera* biomass with sediment total phosphorus.

3.9. Zostera Biomass Relationship with Sediment Total Phosphorus

By assuming the *Zostera* biomass and sediment total phosphorus in Lake Illawarra (the location of the lagoon is shown in *Figure 1.2, page 11 in* Harris (1977), 34°32′32.2″S, 150°49′32.8″E) gives an approximation to Lake Munmorah biomass, the data from Harris (1977), in the summary Table I, was used to develop the relationship shown in Fig. 14.

The relationship obtained was:

$$\text{Zostera biomass}\left(\text{g dw m}^{-2}\right) = 2.031 \times \text{Sediment totalphosphorus}\left(\mu\text{g gdw}^{-1}\right) - 112.83 \quad (12)$$

$R^2 = 0.8469$, n = 18, p > 0.001.

The Fig. 14 shows that a sediment TP < about 55 µg gdw^{-1} may not have influenced water temperature and light intensity quadratic relationships with G_{net} at the MF sampling site selected by Holland (1982) to provide relatively natural conditions, and likely provided baseline conditions for *Zostera* growth rates. Hence, the probable low TP may explain the higher variability, without heatwave effects in November and December, of the biomass at MF in Fig. 12, compared to the more stable and higher biomass, with two southern winter and 5 summer surveys, in the urbanized areas of Lake Munmorah in Fig. 13.

The likely higher TP input to Lake Munmorah was estimated from the average biomass of 28.1 g dw m^{-2} in Fig. 13 by (12) as about 69 ([28.1 + 112.83]/2.031) µg gdw^{-1}, a moderate TP at the low end of the range in Fig. 13. As the maximum G_{net} at MF 13.4 was related to the upper biomass, the same may have occurred in Lake Munmorah, so the TP required to increase maximum G_{net} to above 17.4 mg gdw^{-1} day^{-1} for the upper biomass was estimated as 74 ([36.7 +112.83]/2.031) µg gdw^{-1}. Although the maximum G_{net} was about 30% higher than at MF, the TP was only about 12% higher, and gave a significant increase in average biomass to 28.1 compared to 12.3 g dw m^{-2} at MF with improved stability. That is an important finding and suggests, with further research, the possibility of maintaining *Zostera* biomass in estuaries and coastal lagoons by control of important catchment nutrient inputs, such as total phosphorus.

4. Discussion

A summary table of the final derived equations is shown in Table III for reference by estuary managers.

Note that the expected error of the data used to draw conclusions was highly accurate for 2nd Order curvilinear growth rates with water temperature, light intensity, and biomass with sediment total phosphorus. The equations were tested by R^2 and statistical p-values, which averaged for Water R^2 0.9305 (range 0.8634 to 0.9889), giving P > 0.001 for all regressions, light intensity averaged R^2 0.9071 (range 0.8601 to 0.9617), p > 0.001 for all, *Zostera* biomass with STP 0.8469, p > 0.001. The *Zostera* biomass with net growth rate was R^2 0.8976, p > 0.01 for n = 6, an adequate overall error of 1.94 gdw/m^2 or 16.4% of the average biomass of 11.83 gdw/m^2.

Recommendations for estuary seagrass managers:

This study found the following key findings: it applies a mathematical, 2nd Order curvilinear solution for the effects of water temperature and light intensity on *Zostera capricorni* growth rates, and a linear sediment total phosphorus on *Zostera* biomass growth rates in coastal lagoons. The aim is that these types of mathematical solutions could be used by estuary managers for other species of *Zostera* and seagrasses known to respond to the main drivers in a similar way. It is likely that further research on this approach will generate new knowledge and insights for seagrass management.

The primary implications for seagrass management are:

- Seagrass modelling theory shows curvilinear relationships of growth rates with water temperature due to the respiration rate exceeding the optimum water temperature and with light intensity due to photo−inhibition at high intensities;
- Effects of recent climate change on water temperature increases of 1.4°C to 28°C in coastal lagoons on *Zostera* growth rates add to the curvilinear effect;
- Linear relationship of *Zostera* biomass with sediment total phosphorus and with net growth rates, giving a benchmark for sediment total phosphorus;
- Seagrass biomass stability was associated with catchment phosphorus input from urbanized areas of the Tuggerah Lakes lagoon systems.
- Further research is suggested to apply these types of mathematical solutions to seagrass in other locations, such as *Zostera* spp., *Halophila* spp. *Syringodium* spp., *Cymodocea* spp., *Halodule* spp., and *Thalassia* spp. as explained in Section 1.4, above.

The key findings are supported by the literature in the Introduction and Methods, with the following literature sources using the subject terminology. To begin, the literature indicates global seagrass restoration requires urgent need in the Mediterranean, Africa, India, Asia and Australia due to environmental degradation of estuaries by catchment runoff (Mwikamba *et al*., 2024, see their Figure 1). Although the most frequent restoration method is by the planting of seeds or roots with attached leaves above the sediment surface, they have limited success and give highly variable results (for example see, van derHeide *et al*., 2007, Boudouresque *et al*., 2021, Garmendia *et al*., 2023). However, Cullen-Unsworth and Unsworth (2016) outlined processes for seagrass management by control of catchment runoff for sediment and nutrient loads to global estuaries. That was followed by Floyd *et al*. (2024) at the Maldives Islands in the Indian Ocean, southwest of India where the estuarine seagrass area significantly increased with reduction in sediment and nutrient loads by properly managed land reclamation.

The study by Qin *et al*. (2021, see their Table I) on *Zostera marina* in Southern Korea showed addition of equal dissolved inorganic concentrations of nitrogen and phosphorus resulted in lower sediment P, and therefore

TABLE III: A Summary Table of the Final Derived Equations

Functional characteristics	Description	Derived equations	Source of data
Fig. 1. Monthly water temperature variations	Water temperature = − 0.0073 × (month since October, 1978)^4 + 0.2778 × (month since October, 1978)^3 − 3.4095 × (month since October, 1978)^2 + 14.289 × (month since October, 1978) + 7.9803	Eq. (1)	Redrawn from Holland (1982) Figure 2.4 "Seasonal variation in water temperature at four field sites in Lakes Munmorah and Budgewoi'.
Fig. 3. Relationship of *Zostera* Gross growth rate with water.	*Zostera* gross growth rate (mg gdw^{-1} day^{-1}) = 1.148 × Water temperature (°C) − 8.3893	Eq. (2)	Gross rates in Table II and temperatures *from Appendix A1* in (Holland, 1982).
Fig. 4. Relationship of *Zostera* loss rate with water temperature.	Zostera loss rate (mg gdw^{-1} day^{-1}) = 0.0143 × e$^{(0.2522 \times T)}$	Eq. (3)	Estimated and adjusted loss rates in Table II and water temperatures in Holland (1982) *Appendix A1*.
Zostera net growth rate	Net growth rate = 1.148 × T − 8.3893 − 0.0143 × e$^{(0.2522 \times T)}$	Eq. (4)	Estimated from (2) and (3).
Fig. 5. The quadratic 2nd Order relationship of net growth rate of Zostera with water temperatures.	Net Growth Rate (mg gdw^{-1} day^{-1}) = −0.1305 × T^2 + 5.5604 × T – 45.569	Eq. (5)	Net growth rates in Holland (1982) *Figure 6.3* "*Comparative growth rates of Zostera capricorni at the four field site. Munmorah Flats*" with Table II October, November, and December, 1979 adjustments. Climate change 1.4°C by Scanes *et al*. (2020). The curve shows the optimum temperature and the maximum net growth rate.
Fig. 6. Respiration rate at the average optimum temperature for *Zostera capricorni*.	Respiration rate (mg gdw^{-1} day^{-1}) = 1.345 × e$^{(0.109 \times T)}$	Eq. (6)	Holland (1982) *Zostera* net rates as measured in *Table 6.1* with the Table II adjustments using the difference between respiration rate, R, and the estimated and adjusted loss rates, L, in Table II.
Fig 7. Seasonal variation of incident light intensities at the Lake Munmorah sampling site modified from *Figure 2.8* "*Temperature, salinity and incident light data for Lake Munmorah*".	Incident light intensities (µmol m^{-2} sec^{-1}) = −0.0694 × (month since October, 1978)^5 + 2.4777 × (month since October, 1978)^4 – 27.509 × (month since October, 1978)^3 + 97.822 × (month since October, 1978)^2 – 117.98 × (month since October, 1978) + 2206.8	Eq. (7)	Modified from Holland (1982) *Figure 2.8* "*Temperature, salinity and incident light data for Lake Munmorah*".
Fig. 8. Seasonal variation light intensities at 0.5m inside the *Zostera* bed at the Lake Munmorah sampling site from October, 1978.	Light intensities at 0.5 m inside the *Zostera* bed = −0.0667 × (month since October, 1978)^5 + 2.4894 × (month since October, 1978)^4 – 29.877 × (month since October, 1978)^3 + 123.68 × (month since October, 1978)^2 – 152.76 × (month since October, 1978) + 1482.8	Eq. (8)	Incident light intensities in *Table 2.2* multiplied by light penetration from *Appendix A1*, page 196 in Holland (1982), with additions and adjustments.
Fig. 9. Relationship of light intensities at 0.5 m (I_d) inside the *Zostera* bed with incident light intensities (I_0).	Light intensity at 0.5 m (I_d) = 0.7109 × incident light intensity (I_0) – 96.469	Eq. (9)	From Holland (1982) incident light intensities (I_0) in *Table 2.2* with measured percent penetration in *Appendix A1*, with estimated I_0 for March and October, 1979 in Table II.
Fig. 10. Quadratic 2nd Order relationship of net growth rate with light intensity at I_d 0.5 m depth in the *Zostera* bed.	Net Growth Rate (mg gdw^{-1} day^{-1}) = −1.40E-05 × I_d^2 + 0.0384 × I_d – 12.944	Eq. (10)	Net growth rates in Holland (1982) *Table 6.1* and adjusted rates for September, 1979 and heatwave affected in Table II.
Fig. 11. Relationship of *Zostera* biomass with net growth rate.	*Zostera capricorni biomass (g dw m^{-2}) = 4.0106 × Net growth rate (mgdw gdw^{-1} day^{-1}) – 32.885*	Eq. (11)	From *Table 5.2* in Holland (1982) with *Table 6.1* net growth rates using the September and October, 1979 adjusted rates in Table II.
Fig. 14. *Zostera* biomass relationship with sediment total phosphorus in Lake Illawarra.	*Zostera* biomass (g dw m^{-2}) = 2.031 × Sediment total phosphorus (µg gdw^{-1}) - 112.83	Eq. (12)	Harris (1977).

lower seagrass growth rates. However, sediment total phosphorus appears important due to empirical evidence of its overriding effects on long-term growth rates and biomass. In that regard, de Boer (2007) showed that some estuaries will have high total phosphorus loads by catchment runoff, causing increased macro-algae growth and increased water turbidity by increased phytoplankton production, which reduces light availability outside seagrass beds with subsequent reduction in seagrass area and biomass. The study by Björk *et al*. (2021) indicated that light intensity may also affect seagrass biomass. The study by Zabarte-Maeztu et al. (2020) suggested that catchment runoff management needs to consider increased land clearing, causing increased suspended sediment load and

increased water turbidity, thereby reducing light intensity inside seagrass beds with subsequent reduction in growth rates and biomass. The long-term water turbidity problem also indicates monitoring could include light conditions by secchi depth measurements outside the deep water extent of the *Zostera* bed because it influences the depth distribution and hence most of the *Zostera* cover area other than the inshore extent (see Hodgson and Bucher (2023), their Figure 11). Although recent seagrass modelling studies are more concerned with recovery of the animals living in seagrass, rather than the seagrass recovery itself, Horn *et al*. (2021) found a curvilinear recovery of mixed beds of *Zostera marina* and *Zostera noltei* after sewage diversion from the bay adjacent to the northern Wadden Sea. They used the well-known Ecopath Model to show the biomass, B, in gC/m^2 and production, P, (estimated by B × (P/B) ratio) recovery from 1990 to 2010 (see their supplementary Table S3: Predicted biomass changes from 1990 to 2010 based on model predictions including seagrass mediation https://onlinelibrary.wiley.com/action/downloadSupplement?doi=10.1111%2Frec.13328&file=rec13328-sup-0002-Tables.docx). The increased seagrass biomass was probably due to a resulting moderate catchment input of suspended sediments and nutrients, particularly total phosphorus, as noted by Hodgson and Bucher (2023). The rate of biomass increase had not flattened out by 2010, probably because the moderate catchment suspended sediment input had not significantly reduced light intensity in the seagrass bed and water temperatures had not reached critical levels in the high latitude of the North Sea. Hence, the importance of estuary managers to obtain moderate levels of catchment inputs for a curvilinear increase in biomass and related net growth rates.

5. Conclusions

This study applies a curvilinear 2nd Order mathematical solution for effects of water temperature, light intensity, and linear for sediment total phosphorus on *Zostera* biomass and net growth rates, and could provide for improved management of *Zostera* growth rates and biomass in estuaries and saline coastal lagoons. Due to the fundamental processes involved, it is likely that similar mathematical solutions apply to other seagrass areas. Hence, the studied factors and potential mitigation measures could generate new knowledge and insights for seagrass management. It is hoped the approach will be of assistance to estuary managers, seagrass researchers, and modelers using the related environmental conditions that support *Zostera* species growth rates and biomass. In addition, a reduction in seagrass growth rates with the climate change water temperature increase indicated the need for carbon emission mitigation measures. For example, Stankovic *et al*. (2021, see their Figure 1) showed the existing seagrass in South-east Asia took up some of the carbon emissions, indicating the potential benefits to atmospheric carbon removal of seagrass biomass rebuilding. That is supported by Duarte *et al*. (2013, see their Table 2), who estimated global seagrass areas deposit about 30% of atmospheric carbon into sediments per year.

Acknowledgment

Comments on the draft manuscript by Danny Bucher and an unknown independent reviewer helped improve the scientific presentation of mathematical solutions with catchment management and assessment of seagrass growth rate and biomass changes. There was no funding for this part of the study, which developed from a conference paper on the curvilinear relationship of *Zostera capricorni* net leaf growth rate with water temperature and long-term studies on seagrass biological processes in saline coastal lagoons.

Conflict of Interest

The authors declare that they do not have any conflict of Interest.

References

ASTM E729-96. (2014). Standard Guide for Conducting Acute Toxicity Tests on Test Materials with Fishes, Macroinvertebrates, and Amphibians. https://www.astm.org/e0729-96r14.html.

Beer, S., & Björk, M. (2000). Measuring rates of photosynthesis of two tropical seagrasses by pulse amplitude modulated (PAM) fluorometry. *Aquat Bot*, *66*, 69–76. https://doi.org/10.1016/S0304-3770(99)00020-0.

Björk, M., Asplund, M. E., Deyanova, D., & Gullström, M. (2021). The amount of light reaching the leaves in seagrass (*Zostera marina*) meadows. *PLoS ONE*, *16*(9), e0257586. https://doi.org/10.1371/journal.pone.0257586.

Boudouresque, C. F., Blanfuné, A., Pergent, G., & Thibaut, T. (2021). Restoration of seagrass meadows in the Mediterranean Sea: A critical review of effectiveness and ethical issues. *Water*, *13*, 1034. https://doi.org/10.3390/w13081034.

Cabaço, S., Machás, R., & Santos, R. (2007). Biomass-density relationships of the seagrass *Zostera noltii*: A tool for monitoring anthropogenic nutrient disturbance. *Estuar Coast Shelf Sci*, *74*, 557–564. https://doi.org/10.1016/j.ecss.2007.05.029.

Cabello-Pasini, A., Muñiz-Salazar, R., & Ward, D. H. (2003). Annual variations of biomass and photosynthesis in *Zostera marina* at its southern end of distribution in the North Pacific. *Aquatic Botany*, *76*, 31–47. https://doi.org/10.1016/S0304-3770(03)00012-3.

Campbell, S. J., Kerville, S. P., Coles, R. G., & Short, F. (2008). Photosynthetic responses of subtidal seagrasses to a daily light cycle in Torres Strait: A comparative study. *Cont. Shelf Res*, *28*, 2275–2281. https://doi.org/10.1016/j.csr.2008.03.038.

Cane, H. V., & Richardson, I. G. (1997). What caused the large geomagnetic storm of November 1978? *Journal of Geophysical Research*, *102*, 17445–17449. https://agupubs.onlinelibrary.wiley.com/doi/pdf/10.1029/97JA01420.

Carr, J. A., D'Odorico, P., McGlathery, K. J., & Wiberg, P. L. (2012). Stability and resilience of seagrass meadows to seasonal and interannual dynamics and environmental stress. *Journal of Geophysical Research: Biogeosciences*, *117*(G01007), 12. https://doi.org/10.1029/2011JG001744.

Chartrand, K. M., Bryant, C. V., Carter, A. B., Ralph, P. J., & Rasheed, M. A. (2016). Light thresholds to prevent dredging impacts on the great barrier reef seagrass, *Zostera muelleri* ssp. *capricorni*. *Frontiers in Marine Science*, *3*(106), 17. https://doi.org/10.3389/fmars.2016.00106.

Cho, H. J., Biber, P., & Nica, C. (2009). The rise of *Ruppia* in *seagrass* beds: changes in coastal environment and research needs. In E. K. Drury, & T. S. Pridgen (Eds.), *Handbook on environmental quality* (pp. 333–348). Nova Science Publishers (Chapter 12). https://aquila.usm.edu/fac_pubs/19833

Collier, C. J., Ow, Y. X., Langlois, L., Uthicke, S., Johansson, C. L., O'Brien, K. R., Hrebien, V., & Adams, M. P. (2017). Optimum temperatures for net primary productivity of three tropical seagrass species. *Frontiers in Plant Science*, *8*, 1446. https://doi.org/10.3389/fpls.2017.01446.

Cullen-Unsworth, L. C., & Unsworth, R. K. (2016). Strategies to enhance the resilience of the world's seagrass meadows. *Journal of Applied Ecology*, *53*(4), 967–972. https://doi.org/10.1111/1365-2664.12637.

de Boer, W. F., (2007). Seagrass-sediment interactions, positive feedbacks and critical thresholds for occurrence: A review. *Hydrobiologia*, *591*, 5–24. https://doi.org/10.1007/s10750-007-0780-9.

Dennison, W. C., & Alberte, R. S. (1985). Role of daily light period in the depth distribution of *Zostera marina* (eelgrass). *Marine Ecology Progress Series*, *25*, 51–61. https://www.int-res.com/articles/meps/25/m025p051.pdf.

Duarte, C. (1990). Seagrass nutrient content. *Marine Ecology Progress Series*, *67*, 201–207. https://www.int-res.com/articles/meps/67/m067p201.pdf.

Duarte, C. M., Losada, I. J., Hendriks, I. E., Mazarrasa, I., & Marbà, N. (2013). The role of coastal plant communities for climate change mitigation and adaptation. *Nature Climate Change*, *3*, 961–968. http://10.1038/NCLIMATE1970.

FAO. (2022). Restoration and the UN Decade on Ecosystem Restoration 2021-2030. https://unosd.un.org/sites/unosd.un.org/files/green_deal_ecosystem_mr._tim_christophersen.pdf.

Fickling, M. D., & Dougherty, L. M. (1983). Solar Activity during 1979. *Journal of the British Astronomical Association*, *94*, 25–28. https://adsabs.harvard.edu/full/1983JBAA.94.25F.

Floyd, M., East, H. K., Traganos, D., Musthag, A., Guest, J. R., Hashim, A. S., Evans, V., Helber, S., Unsworth, R. K. F., & Suggitt, A. J. (2024). Rapid seagrass meadow expansion in an Indian Ocean bright spot. *Scientific Reports*, *14*, 10879. https://doi.org/10.1038/s41598-024-61088-1.

Fong, P., Jacobson, M. E., Mescher, M. C., Lirman, D., & Harwell, M. C. (1997). Investigating the management potential of a seagrass model through sensitivity analysis and experiments. *Ecological Applications*, *7*, 300–315. https://www.jstor.org/stable/2269425.

Garmendia, J. M., Rodríguez, J. G., Borja, Á., Pouso, S., del Campo, A., Galparsoro, I., & Fernandes-Salvador, J. A. (2023). Restoring seagrass meadows in Basque estuaries: Nature-based solution for successful management. *Nature-Based Solutions*, *4*, 100084. https://doi.org/10.1016/j.nbsj.2023.100084.

George, R., Gullström, M., Mangora, M. M., Mtolera, M. S. P., & Björk, M. (2018). High midday temperature stress has stronger effects on biomass than on photosynthesis: A mesocosm experiment on four tropical seagrass species. *Ecology and Evolution*, *8*, 4508–4517. https://doi.org/10.1002/ece3.3952.

Harris, M. McD. (1977). cological Studies on Illawarra Lake with Special Reference to *Zostera capricorni* Ascherson. Master of Science Thesis, School of Botany, University of New South Wales, Sydney, Australia. https://doi.org/10.26190/unsworks/20231.

Hodgson, B. R., & Bucher, D. J. (2023). Biological processes in seagrass beds of coastal lagoons to maintain estuary-dependent marine fisheries. *Marine Environmental Research*, *189*, 106033. https://doi.org/10.1016/j.marenvres.2023.106033.

Holland, V. M. (1982). The effects of some environmental factors on the growth and viability of Zostera capricorni Asherson. M.Sc. Thesis, School of Botany, University of New South Wales, Sydney, Australia. https://doi.org/10.26190/unsworks/7044

Horn, S., Coll, M., Asmus, H., & Dolch, T. (2021). Food web models reveal potential ecosystem effects of seagrass recovery in the northern Wadden Sea. *Restoration Ecology*, *29*, e13328. https://doi.org/10.1111/rec.13328.

Ives, A. R., Dennis, B., Cottingham, K. L., & Carpenter, S. R. (2003). Estimating community stability and ecological interactions from time series data. *Ecological Monographs*, *73*, 301–330. https://doi.org/10.1890/0012-9615(2003)073.

Jakeman, A. J., Letcher, R. A., & Norton, J. P. (2006). Ten iterative steps in development and evaluation of environmental models. *Environmental Modelling and Software*, *21*, 602–614. https://doi.org/10.1016/j.envsoft.2006.01.004.

Kaldy, J. E. (2014). Effect of temperature and nutrient manipulations on eelgrass *Zostera marina* L. from the Pacific Northwest, USA. *Journal of Experimental Marine Biology and Ecology*, *453*, 108–115. https://doi.org/10.1016/j.jembe.2013.12.020.

King, R. J., & Hodgson, B. R. (1986). Aquatic angiosperms in coastal saline lagoons of New South Wales. IV. Long-term changes. *Proceedings of the Linnean Society of New South Wales*, *109*, 51–60. https://www.biodiversitylibrary.org/page/35125308#page/63/mode/1up.

King, R. J., & Holland, V. M. (1986). Aquatic angiosperms in coastal saline lagoons of New South Wales II. The Vegetation of Tuggerah Lakes, with Specific Comments on the Growth of *Zostera capricorni* Ascherson. *Proceedings of the Linnean Society of New South Wales*, *109*, 25–39. https://www.biodiversitylibrary.org/page/35125282#page/37/mode/1up.

Koedsin, W., Intararuang, W., Ritchie, R. J., & Huete, A. (2016). An integrated field and remote sensing method for mapping seagrass species, cover, and biomass in southern Thailand. *Remote Sensing*, *8*(4), 292. https://doi.org/10.3390/rs8040292.

Lee, K. S., Park, S. R., & Kim, Y. K. (2007). Effects of irradiance, temperature, and nutrients on growth dynamics of seagrasses: A review. *Journal of Experimental Marine Biology and Ecology*, *350*, 144–175. https://doi.org/10.1016/j.jembe.2007.06.016.

Lillebø, A. I., Neto, J. M., Martins, I., Verdelhos, T., Leston, S., Cardoso, P. G., Ferreira, S. M., Marques, J. C., & Pardal, M. A. (2005). Management of a shallow temperate estuary to control eutrophication: The effect of hydrodynamics on the system's nutrient loading. *Estuarine Coastal and Shelf Science*, *65*, 697–707. https://doi.org/10.1016/j.ecss.2005.07.009.

Moore, K. A., Neckles, H. A., & Orth, R. J. (1996). *Zostera marina* (eelgrass) growth and survival along a gradient of nutrients and turbidity in the lower Chesapeake Bay. *Mar Ecol Prog Ser*, *142*, 247–259. https://www.int-res.com/articles/meps/142/m142p247.pdf.

Mwikamba, E. M., Githaiga, M. N., Briers, R. A., & Huxham, M. (2024). A review of seagrass cover, status and trends in Africa. *Estuaries and Coasts*, *47*, 917–934. https://doi.org/10.1007/s12237-024-01348-5.

Neckles, H. A., Kopp, B. S., Peterson, B. J., & Pooler, P. S. (2012). Integrating scales of seagrass monitoring to meet conservation needs. *Estuaries and Coasts*, *35*, 23–46. https://doi.org/10.1007/s12237-011-9410-x.

Nguyen, H. M., Ralph, P. J., Marín-Guirao, L., Pernice, M., & Procaccini, G. (2021). Seagrasses in an era of ocean warming: a review. *Biological reviews*, *96*, 2009–2030. https://doi.org/10.1111/brv.12736.

Nielsen, S. L., Sand-Jensen, K., Borum, J., & Geertz-Hansen, O. (2002). Depth colonization of eelgrass (Zostera marina) and macroalgae as determined by water transparency in Danish coastal waters. *Estuaries*, *25*, 1025–1032. https://doi.org/10.1007/BF02691349.

Patrićio, J., & Marques, J. C. (2006). Mass balanced models of the food web in three areas along a gradient of eutrophication symptoms in the south arm of the Mondego estuary (Portugal). *Ecological Modelling*, *197*, 21–34. https://doi.org/10.1016/j.

Plaisted, H. K., Shields, E. C., Novak, A. B., Peck, C. P., Schenck, F., Carr, J., Duffy, P. A., Evans, N. T., Fox, S. E., Heck, S. M., & Hudson, R. (2022). Influence of rising water temperature on the temperate seagrass species eelgrass (*Zostera marina* L.) in the Northeast USA. *Frontiers in Marine Science*, *9*, 920699. https://doi.org/10.3389/fmars.2022.920699.

Plus, M., Chapelle, A., Ménesguen, A., Deslous-Paoli, J.-M., & Auby, I. (2003). Modelling seasonal dynamics of biomasses and nitrogen contents in a seagrass meadow (*Zostera noltii* Hornem.): Application to the Thau lagoon (French Mediterranean coast). *Ecological Modelling*, *161*, 213–238. https://doi.org/10.1016/S0304-3800(02)00350-2.

Qin, L., Suonan, Z., Kim, S. H., & Lee, K. (2021). Growth and reproductive responses of the seagrass *Zostera marina* to sediment nutrient enrichment. *ICES Journal of Marine Science*, *78*, 1160–1173. https://doi.org/10.1093/icesjms/fsab031.

Saborowski, R., & Hünerlage, K. (2022). Hatching phenology of the brown shrimp *Crangon crangon* in the southern North Sea: Interannual temperature variations and climate change effects. *ICES Journal of Marine Science*, *79*, 1302–1311. https://doi.org/10.1093/icesjms/fsac054.

Santamaŕia, L., & van Vierssen, W., (1997). Photosynthetic temperature responses of fresh- and brackish-water macrophytes a review. *Aquatic Botany*, *58*, 135–150. https://doi.org/10.1016/S0304-3770(97)00015-6.

Scalpone, C. R., Jarvis, J. C., Vasslides, J. M., Testa, J. M., & Ganju, N. K. (2020). Simulated estuary-wide response of seagrass (*Zostera marina*) to future scenarios of temperature and sea level. *Frontiers in Marine Science*, *7*, 539946. https://doi.org/10.3389/fmars.2020.539946.

Scanes, E., Scanes, P. R., & Ross, P. M. (2020). Climate change rapidly warms and acidifies Australian estuaries. *Nature Communications*, *11*(1), 1803. https://doi.org/10.1038/s41467-020-15550-z.

Shields, E. C., Moore, K. A., & Parrish, D. B. (2018). Adaptations by Zostera marina dominated seagrass meadows in response to water quality and climate forcing. *Diversity*, *10*, 125. https://doi.org/10.3390/d10040125.

Short, F. T. (1980). A simulation model of the seagrass production system. In R. C. Phillips, & C. P. McRoy (Eds.), *Handbook of seagrass biology: An ecosystem perspective* (Chapter 15, pp. 277–295). Garland, New York: STPM Press. https://www.researchgate.net/profile/Frederick-Short/publication/259382867_A_simulation_model_of_the_seagrass_production_system/links/0c96052b46bd764d9e000000/A-simulation-model-of-the-seagrass-production-system.pdf

Stankovic, M., Ambo-Rappe, R., Carly, F., Dangan-Galon, F., Fortes, M. D., Hossain, M. S., Kiswara, W., Van Luong, C., Minh-Thu, P., Mishra, A. K., & Noiraksar, T. (2021). Quantification of blue carbon in seagrass ecosystems of Southeast Asia and their potential for climate change mitigation. *Science of the Total Environment*, *783*, 146858. https://doi.org/10.1016/j.scitotenv.2021.146858.

Thomas, C., Hart, B., Nicholson, A., Grace, M., Brodie, J., & Pollino, C. (2005). Development of criteria for simplifying ecological risk models. *MODSIM05 International Conference on Modelling and Simulation, 12-15 December 2005*, Melbourne, pp. 772–778. https://www.mssanz.org.au/modsim05/papers/thomas.pdf

Unsworth, R., Nordlund, L., & Cullen-Unsworth, L. (2018). Seagrass meadows support global fisheries production. *Conservation Letters*, *12*, e12566. https://doi.org/10.1111/conl.12566.

van derHeide, T., van Nes, E. H., Geerling, G. W., Smolders, A. J., Bouma, T. J., & van Katwijk, M. M., (2007). Positive feedbacks in seagrass ecosystems: Implications for success in conservation and restoration. *Ecosystems*, *10*, 1311–1322. https://doi.org/10.1007/s10021-007-9099-7.

Verhagen, J. H. G., & Nienhuis, P. H. (1983). A simulation model of production, seasonal changes in biomass and distribution of eelgrass (*Zostera marina*) in Lake Grevelingen. *Marine Ecology Progress Series*, *10*, 187–195. https://doi.org/10.1007/BF02255383.

Zabarte-Maeztu, I., Matheson, F. E., Manley-Harris, M., Davies-Colley, R. J., Oliver, M., & Hawes, I. (2020). Effects of fine sediment on seagrass meadows: A case study of Zostera muelleri in Pāuatahanui Inlet, New Zealand. *Journal of Marine Science and Engineering*, *8*(9), 645. https://doi.org/10.1016/j.marenvres.2021.105480.

Zhang, Y. H., Li, J. D., Wu, Z. X., Yuan, S. J., Li, W. T., & Zhang, P. D. (2022). Effects of different prolonged light durations on survival, growth and physiology of the eelgrass Zostera marina. *Frontiers in Environmental Science*, *10*, 893377. https://doi.org/10.3389/fenvs.2022.893377.